Ecosystems Mission Area—Species Management Research Program

Status, Trend, and Monitoring Effectiveness of Marbled Murrelet (*Brachyramphus marmoratus*) at Sea Abundance and Reproductive Output off Central California, 1999–2021

Open-File Report 2023–1065

U.S. Department of the Interior
U.S. Geological Survey

Cover. A pair of marbled murrelets (*Brachyramphus marmoratus*) observed offshore of Santa Cruz, California, July 1, 2014. Photograph by Alex Rinkert, U.S. Geological Survey.

Status, Trend, and Monitoring Effectiveness of Marbled Murrelet (*Brachyramphus marmoratus*) at Sea Abundance and Reproductive Output off Central California, 1999–2021

By Jonathan Felis, Josh Adams, and Benjamin Becker

Ecosystems Mission Area—Species Management Research Program

Open-File Report 2023–1065

U.S. Department of the Interior
U.S. Geological Survey

U.S. Geological Survey, Reston, Virginia: 2023

For more information on the USGS—the Federal source for science about the Earth, its natural and living resources, natural hazards, and the environment—visit https://www.usgs.gov or call 1–888–392–8545.

For an overview of USGS information products, including maps, imagery, and publications, visit https://store.usgs.gov/ or contact the store at 1–888–275–8747.

Suggested citation:
Felis, J., Adams, J., and Becker, B., 2023, Status, trend, and monitoring effectiveness of Marbled Murrelet (*Brachyramphus marmoratus*) at sea abundance and reproductive output off central California, 1999–2021: U.S. Geological Survey Open-File Report 2023–1065, 47 p., https://doi.org/10.3133/ofr20231065.

Associated data for this publication:
Felis, J.J., Adams, J., Peery, M.Z., Henry, R.W., Henkel, L.A., Becker, B.H., and Halbert, P., 2022, Annual marbled murrelet abundance and productivity surveys off central California (Zone 6), 1999–2021 (ver. 4.0, May 2022): U.S. Geological Survey data release, https://doi.org/10.5066/F75B01RW.

ISSN 2331-1258 (online)

Acknowledgments

We would like to thank current and former investigators and field crew that have collected and stewarded the data evaluated herein: Kira Arias, Jessie Beck, Marika Bordeaux, Abe Borker, Ryan Carle, Emily Coletta, Max Czapanskiy, Parker Forman, Jared Figurski, Portia Halbert, Laurie Hall, Laird Henkel, Bill Henry, Cheryl Horton, Emma Kelsey, Caitlin Kroeger, Ben Moran, Zach Peery, Alex Rinkert, Zeke Smith, Jennilyn Stenske, Joelle Sweeney, Breck Tyler, and Laney White. Logistical support has been made possible throughout the years by the U.C. Santa Cruz small boat program (Dave Benet); U.S. Geological Survey Western Ecological Research Center, Pacific Coastal and Marine Science Center, and Marine Facility crews (Tim Elfers, Cordell Johnson, SeanPaul La Selle, Jackson Currie, Morgan Gilmour, and Rob Wyland). This work was funded by California State Parks, and annual field surveys were funded by the U.S. Fish and Wildlife Service Natural Resource Damage Assessment and Restoration Program and the Luckenbach Oil Spill Trustee Council. We are grateful to Scott Pearson and Mayumi Arimitsu for reviewing earlier versions of this report.

Contents

Figures

Tables

Conversion Factors

International System of Units to U.S. customary units

Multiply	By	To obtain
	Length	
meter (m)	3.281	foot (ft)
kilometer (km)	0.6214	mile (mi)
kilometer (km)	0.5400	mile, nautical (nmi)
meter (m)	1.094	yard (yd)
	Area	
square kilometer (km^2)	247.1	acre
square kilometer (km^2)	0.3861	square mile (mi^2)

Abbreviations

AHY after-hatch-year

AIC Akaike information criterion

CI confidence interval

CV coefficient of variation

DSM density surface model

df degrees of freedom

GAM generalized additive model

GLM general linear model

GPS Global Positioning System

HY hatch-year

p probability value

t t-statistic

SE standard error

Status, Trend, and Monitoring Effectiveness of Marbled Murrelet (*Brachyramphus marmoratus*) at Sea Abundance and Reproductive Output off Central California, 1999–2021

By Jonathan Felis[1], Josh Adams[1], and Benjamin Becker[2]

Abstract

Marbled Murrelets (*Brachyramphus marmoratus*) have been listed as "endangered" by the State of California and "threatened" by the U.S. Fish and Wildlife Service since 1992 in California, Oregon, and Washington. Information regarding murrelet abundance, distribution, and habitat associations is critical for risk assessment, effective management, evaluation of conservation efficacy, and ultimately, the meeting of Federal- and State-mandated recovery efforts. From 1999 to present, line-transect surveys have been performed to estimate at-sea abundance and reproductive output of Marbled Murrelets in the marine environment in U.S. Fish and Wildlife Service Conservation Zone 6 (San Francisco Bay to Point Sur in central California). Using this long-term annual time series, we developed a new and comprehensive analytical framework to estimate annual murrelet abundance and trend at sea, evaluated the effectiveness of spatial and temporal components of the monitoring study design, assessed two measures of annual murrelet reproductive output, and developed new spatial models to map murrelet at-sea density and estimate model-based annual at-sea abundances. The long-term average, design-based after-hatch-year (AHY) abundance estimate for the study area was 376 murrelets (range: 163–586 annually), and we did not detect any significant trend during the 23 years of monitoring. Spatial-model-based AHY abundance estimates were similar to design-based estimates but with smaller estimated variance. The AHY murrelets were most abundant nearshore, with little annual variation; alongshore, distribution was more annually variable, and some long-term hotspots occurred, particularly around Point Año Nuevo. The AHY murrelet densities were greatest in July and least in June and August. The long-term average hatch-year (HY) abundance estimate was 13 murrelets (range: 0–31 annually), and the long-term average HY:AHY ratio was 0.052; both metrics indicated similar interannual patterns. Evidence of a significant trend in either metric of reproductive output was not detected; although large overlap among interannual abundance and ratio estimates at the 95-percent confidence interval level made it difficult to evaluate interannual differences. Despite the apparent long-term stability in murrelet abundance in this region from 1999 to 2021, future long-term annual monitoring at sea will be critical to determine if the large-scale August 2020 CZU Santa Cruz Mountain wildfire that occurred adjacent to our study area affects local murrelet at-sea abundance and distribution. We also evaluated potential changes to survey and analytical design that could benefit this monitoring program in the future. Results indicated that eliminating the offshore stratum, focusing more effort on the nearshore stratum, and doing fewer surveys focused on a narrower timeframe could maintain or improve AHY trend estimates while preserving the ability to compare them to past years.

Introduction

The Marbled Murrelet (*Brachyramphus marmoratus*; hereafter, "murrelet") is a small, diving seabird of the Alcidae family that inhabits North American nearshore marine waters from Alaska to central California (Nelson, 2020). In California, Marbled Murrelets nest solitarily from March to October (primarily from April to August) in forests within 80 kilometers (km) of the coast (Nelson, 2020). The southernmost known breeding area for Marbled Murrelets is south of San Francisco Bay in the Santa Cruz Mountains and is separated from the nearest northern California nesting population by 240–320 km (fig. 1). During their breeding season, the at-sea distribution of murrelets in this region extends mostly from Half Moon Bay to Santa Cruz, with greatest abundance typically in the waters near Point Año Nuevo (fig. 1; Henry, 2017). Sightings of Marbled Murrelets north or south of this region during the breeding season are less frequent (Ralph and Miller, 1995; Henkel, 2004; eBird, 2021).

[1]U.S. Geological Survey, Western Ecological Research Center, Santa Cruz, Calif.

[2]Californian Cooperative Ecosystem Studies Unit, National Park Service and U.C. Berkeley, Berkeley, Calif.

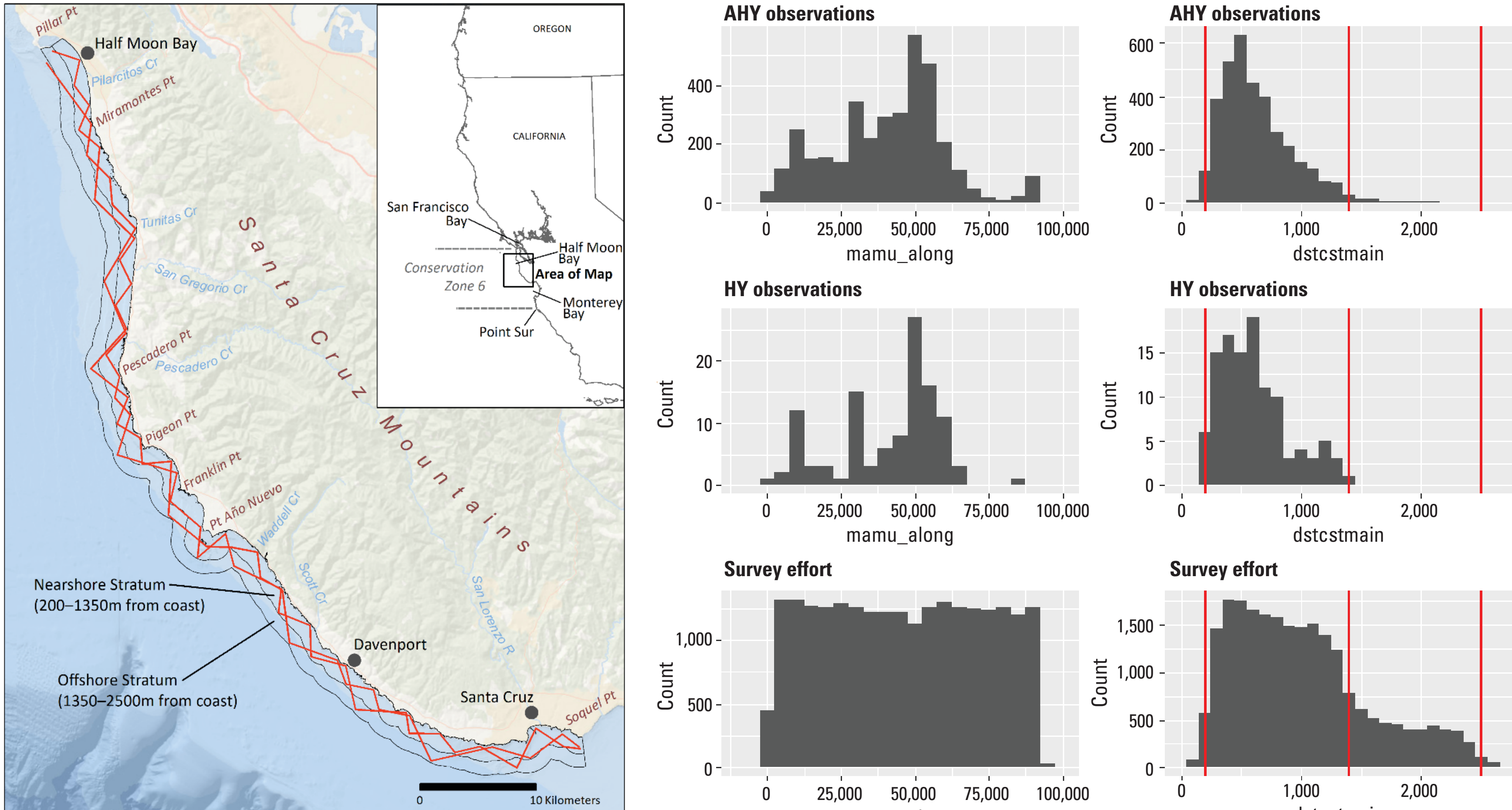

Base map from Esri and its licensors, copyright 2022

Figure 1. Left: Marbled Murrelet Conservation Zone 6 study area, central California, showing nearshore (200–1,350 meters [m] from coast) and offshore (1,350–2,500 m from coast) strata; example randomized zig-zag survey transects are shown in red, with four-times-greater linear effort in the nearshore stratum. Right: Histograms of 1999–2021 murrelet after-hatch-year (AHY) observations (top row), hatch-year (HY) observations (middle row), and survey effort (count of 500-m trackline segments; bottom row) for alongshore position (left column) and distance to mainland coast (right column). Alongshore location is quantified from Half Moon Bay (0, left side of *x*-axis) to Santa Cruz (right side of *x*-axis). Vertical red lines in distance to coast plots indicate design-based boundaries for nearshore and offshore strata.

Murrelets were listed as “endangered” by the State of California (California Department of Fish and Wildlife, 2021) and “threatened” by the U.S. Fish and Wildlife Service (USFWS) in 1992 in California, Oregon, and Washington (U.S. Fish and Wildlife Service, 2021). The USFWS Marbled Murrelet Recovery Plan (U.S. Fish and Wildlife Service, 1997) established six conservation zones for long-term monitoring and recovery efforts; the waters off the Santa Cruz Mountains are at the center of the southernmost conservation zone (Zone 6), which extends from San Francisco Bay to Point Sur (about 225 km of coastline; fig. 1). Abundance of murrelets has been estimated at sea along an 85-km length of coastline adjacent to the Santa Cruz Mountains in Zone 6 since 1999 (excluding 2004–06), with annual estimates of 174–699 individuals at sea (Felis and others, 2022a). The most recent at-sea abundance estimates for Conservation Zones 1–5 combined (19,700 murrelets in 2020; Washington–northern California) and for California (3,870 murrelets in 2021, not including Zone 6; McIver and others, 2022), indicate that Zone 6 represents about 2 percent of the listed range (Washington, Oregon, and California) and about 11 percent of the California abundance (based on 1999–2021 long-term average of 485 murrelets in Zone 6, as reported in Felis and others [2022a]). Abundance at sea has decreased in Washington and increased in Oregon and northern California, with no net change in the overall abundance north of Zone 6 for the last 20 years (McIver and others, 2022). The long-term abundance trend in Zone 6 has not been recently assessed or reported.

Information regarding murrelet abundance, distribution, and habitat associations is critical for risk assessment, effective management, evaluation of conservation efficacy, and ultimately, the meeting of Federal- and State-mandated recovery efforts. The USFWS Recovery Plan for this species (U.S. Fish and Wildlife Service, 1997) indicates a criterion of “stable or increasing populations in four of the six conservation zones” for potential delisting. At-sea abundance and productivity monitoring of Marbled Murrelets in Zone 6 originally served two purposes: (1) to quantify the status of murrelets in central California as part of the USFWS Recovery Plan and (2) to help evaluate murrelet response to ongoing recreational use management and corvid control in coastal California State and County parks (Halbert and Singer, 2017). More recently, the CZU Lightning Complex wildfire burned large areas of murrelet nesting habitat in the Santa Cruz Mountains in August–September 2020 (CAL FIRE, 2021); changes in local breeding murrelet population size and reproductive output in the wake of this habitat loss are now important conservation and management concerns. Finally, quantifying Marbled Murrelet distribution at sea may help resource managers identify and designate critical at-sea habitat for the species (Bellefleur and others, 2009).

In this study, we (1) develop a new and comprehensive analytical framework to estimate annual murrelet abundance and trend consistently for 1999–present; (2) evaluate spatial and temporal components of murrelet density as they pertain to the effectiveness of the study design used for monitoring abundance; (3) estimate and assess multiple measures of annual murrelet reproductive output; and (4) develop new spatial models to map murrelet at-sea density and estimate spatial-model-based annual at-sea abundances. Finally, we use the results to assess potential changes and improvements to study design going forward while maintaining the ability to compare with past years.

Methods

At-Sea Survey Design

Preliminary studies of murrelet distribution and density at sea in Zone 6 (Becker and others, 1997) and survey design simulations based on those results (Rachowicz and others, 2006) determined that a stratified, random, zig-zag survey design, with greater nearshore than offshore effort, would minimize bias for estimating abundance while maximizing power to detect interannual trend. As a result, approximately 60 random and unique survey routes were designed by Becker and Beissinger (2003) and Peery and others (2007). These routes were surveyed in 1999–2003 as continuous, approximately 100-km-long zig-zag transect lines to sample nearshore (200–1,350 meters [m] from coast) and offshore (1,350–2,500 m from coast) strata, with approximately four-times-greater-effort within the nearshore stratum to accommodate greater murrelet densities nearshore (fig. 1). Survey routes used from 2007 to 2021 were randomly selected, without replacement within year, from the original pool of unique routes. An equal number of routes were drawn using starting points at the north and south ends of the survey area. Survey routes that were drawn from the south typically resulted in a greater amount of habitat surveyed within south-facing, leeward bays (for example, Año Nuevo Bay) that often have greater relative abundances of Marbled Murrelets than more exposed stretches of the coast (Henry, 2017); annual surveys typically included an equal number of routes drawn from north and south, except during 1999–2000 when only routes drawn with northern starting points were used.

Surveys were always completed between June 1 and August 24 to capture the murrelet nesting and fledging season (Henry, 2017). From 2001 to 2003, 12–15 surveys were completed annually, and for all other years, an average of 7 surveys (range: 4–9) were completed annually (table 1). Beginning in 2014, the number of surveys done per year was standardized to nine surveys, with three surveys between June 1 and July 9 and six surveys from July 10 to August 24 (appendix 1, table 1.1; fig. 1.1). More effort was devoted to the later survey period to increase juvenile murrelet encounter rates because they are more likely to be observed at sea post-fledging (Peery and others, 2007; see “Hatch-Year Abundance Estimates and Productivity Indices”).

Table 1. Annual numbers of surveys completed, total count of after-hatch-year (AHY) murrelets (and number of unique group detections), percent of AHY murrelets observed on water (excluding flying birds), percent of AHY birds detected in the nearshore stratum, and total count of hatch-year (HY) murrelets for all standardized zig-zag Marbled Murrelet (*Brachyramphus marmoratus*) surveys completed in central California Conservation Zone 6 (Half Moon Bay to Santa Cruz, CA) from 1999 to 2021, during the June 1–August 24 survey season.

[Note that all HY murrelets occurred singly or grouped with AHY murrelets, all were observed on the water (not flying), and all were in the nearshore stratum. See appendix 1, table 1.1 for information on individual surveys. **Abbreviation**: %, percentage]

Year	Number of surveys	Total AHY birds (detections)	AHY % on water	AHY % nearshore	Total HY murrelets
1999	5	223 (129)	96.9	98.7	6
2000	8	318 (180)	91.2	98.7	5
2001	15	796 (432)	95.0	98.4	20
2002	15	727 (407)	95.2	99.3	15
2003	12	603 (339)	92.4	98.2	10
2007	4	141 (82)	79.4	95.7	2
2008	4	60 (35)	90.0	96.7	0
2009	8	401 (236)	93.5	97.8	4
2010	7	341 (203)	81.8	94.1	8
2011	6	180 (110)	92.2	98.3	5
2012	6	240 (137)	90.4	97.9	2
2013	6	336 (194)	78.6	98.2	16
2014	9	398 (221)	89.9	98.0	15
2015	9	247 (143)	94.7	97.6	4
2016	7	325 (172)	98.5	99.7	11
2017	9	333 (195)	86.8	91.6	3
2018	9	235 (141)	86.0	97.0	4
2019	8	222 (130)	87.8	93.7	3
2020	9	300 (174)	96.3	99.3	3
2021	9	224 (128)	86.6	97.3	4

Field Survey Methods and Data Collection

We completed surveys from a small boat using line-transect and distance sampling methods (Becker and others, 1997; Buckland and others, 2001). Two observers, on either side of an open boat, recorded the observation time, angle off the transect line, distance from the vessel, and group size for all murrelets detected. Perpendicular distances for each detection were calculated later as the sine of the sighting angle multiplied by observation distance, where the sighting angle is relative to the direction the boat is traveling. The boat was operated by a third crew member whose sole responsibility was piloting the boat along the transect line. From 1999 to 2003, surveys were done in a 4-m open inflatable skiff at approximately 18 km (10 nautical miles per hour [kts]) per hour. From 2007 to present, a 6-m open skiff (Boston Whaler Guardian 20 or similar) was used at speeds of 22–28 km (11–15 kts) per hour. We performed all surveys by following the selected route from north (Half Moon Bay) to south (Soquel Point, Monterey Bay) using a Global Positioning System (GPS; fig. 1). If the survey route intersected land or crossed hazardous areas (for example, high surf areas or extensive kelp beds nearshore), we maintained the survey effort while safely navigating as close as possible to the transect line. Although most surveys (96 percent) were performed in 1 day, seven surveys were done during 2 consecutive days (three surveys in 1999, one survey in 2001, and three surveys in 2002; appendix 1, table 1.1). Surveys were almost exclusively completed when viewing conditions were excellent to good based on wind, sea state, swell, and glare (appendix 1, table 1.2), and all surveys were initiated within 2 hours after sunrise.

Observers counted murrelets as a group when individuals were within 2 m of each other or if they showed behavior indicative of group status (for example, co-diving or vocalizing with one another; Strong and others, 1995). Observers recorded the age-class of each Marbled Murrelet based on plumage ("after-hatch-year" [AHY] or "hatch-year" [HY]). The vessel occasionally paused or deviated from the transect line to assess Marbled Murrelet age-class; no additional observations were counted when deviating off the transect line. Behavior was recorded as "resting" on the water or "flying." Distances to each group were recorded in meters, and to maintain accurate distance estimates, observers practiced distance estimation using a laser rangefinder on buoys and other targets in the harbor before each survey. Historical protocol (1999–2003) stated that flying birds should only be counted if they crossed the beam of the vessel, and the distance and angle to flying birds was estimated at that time (90-degree angle and a distance estimate; Henry and Tyler, 2017). Re-examination of historical data (Felis and others, 2022b) showed that this protocol was followed in earlier years (1999–2003), but in later years (2007–16), flying birds were given a distance/angle estimate when first detected, although it was unclear if birds were only counted if they crossed the beam. From 2017 to present, we estimated distance and angle to flying birds at the time of first sighting and counted them whether or not they crossed the beam of the vessel. Flying birds were removed in subsequent analyses (see "Detection Function Modeling" and "After-Hatch-Year Abundance Estimates" for further detail).

Observers recorded all observations and observation times using digital voice recorders, including survey start and end times, ocean and viewing conditions (appendix 1, table 1.2), and periods when effort was paused for any reason (for example, vessel deviated from the transect line to identify Marbled Murrelet age-class). After completing a survey, each observer transcribed and reviewed their own recorded data, and these data were merged into a spreadsheet that was examined for quality assurance and quality control (Felis and others, 2022b). From 2017 to present, we acquired a continuous 1-second GPS track during each survey using a handheld GPS unit; this track was used to georeference observations based on matching date and time using custom scripting in R (R Core Team, 2016). From 2007 to 2016, a GPS track was usually collected but at a lower resolution (typically a 30-second interval), and from 1999 to 2003, a GPS track was not collected; during 1999–2016, murrelet observation locations were obtained by collecting a GPS waypoint for each observation.

We created a spatial representation of nearshore and offshore strata in ArcGIS based on a coastline shapefile (California Department of Fish and Wildlife, 2004) and calculated linear effort for each survey within the nearshore and offshore strata by using the drawn survey route in ArcGIS. We assigned Marbled Murrelet observations to each stratum based on location. Historical analyses and abundance estimates (1999–2003) were originally done with an older- and courser-resolution coastline representation (Peery and others, 2006). For our reanalysis, we used the more recent higher-resolution coastline representation to delineate strata and standardize interannual estimates. All observation data, survey routes, survey tracks, and survey metadata used herein are compiled in a publicly available data release (Felis and others, 2022b).

Detection Function Modeling

To estimate the density and abundance of murrelets, we corrected murrelet observations for imperfect detection as a function of distance from the survey transect line using detection function modeling (Buckland and others, 2001) with the "Distance" package in R (Miller and others, 2019). We evaluated hazard rate and half-normal key function detection models using continuous perpendicular observation distances from all years pooled for each age class separately, with and without covariates. For AHY murrelets, we included models with Year as a factor covariate to account for differences in survey crews and vessels among years and because our goal was to produce annual abundance estimates. This multi-covariate distance-sampling approach used the complete dataset to provide information about the shape of the detection function, and covariate-level data were used to fit the scale for each level of the covariate (Year in this case; Marques and others, 2007). Including Year as a covariate creates a simpler and more consistent modeling framework than making a separate model for each year as would be the case in "fully stratified" conventional distance sampling; it also should decrease variance by increasing sample size. For HY murrelets, there were insufficient annual observations to include Year as a covariate; therefore, we included Vessel as a two-level covariate to account for a smaller/slower vessel in 1999–2003 and a larger/faster vessel in 2007–present. For models with no covariate, we allowed cosine expansion with the expansion order allowed to vary automatically and be selected by the "Distance" package in R.

Because of historical inconsistencies in how or when flying murrelets were recorded (see "Field Survey Methods and Data Collection"), we removed flying murrelets from analysis (2–21 percent of observations annually; table 1). We then truncated observations to 100-m perpendicular distance from the transect line; this adjustment resulted in the removal of 6 percent of observations for each age class for all years combined, which followed Buckland and others (2001) recommendation of 5–10 percent truncation of the farthest locations recorded. We ultimately used a total of 3,219 detections of 5,678 AHY murrelets in our analysis (table 1). We limited HY detection function modeling to surveys done within the "juvenile window" (June 10–August 24) as defined by Peery and others (2007) for HY:AHY ratio estimation (see "Hatch-Year Abundance Estimates and Productivity Indices"), resulting in 108 HY murrelet detections used in analysis (table 1). We inspected probability of detection, goodness of fit, and precision for each model to ensure reasonable results and selected the model with the lowest Akaike information criterion (AIC) for each age class.

Previous detection function modeling using these data was done differently and with less consistency. All previous work modeled unique detection functions annually (except for 2008, when observations were too few to model a year-specific detection function and a pooled 2007–08 model was applied to 2008 data), and all model evaluations were limited to the half-normal key function. Peery and others (2006) allowed for covariates that might affect detection probability (observer, view conditions) in annual detection function model selection from 1999 to 2003, but this practice was not used from 2007 to 2021 (Felis and others, 2022a). Additionally, binned detection distances, instead of continuous data, were used in all years, but binning schemes changed throughout time (Felis and others, 2022a). Binning distances into groups for detection function modeling is sometimes used to accommodate systematic errors in field data collection, such as "heaping" of data due to preferential rounding of angles and distances (for example, 0 m, 5 m, 10 m, 15 m…), but this practice can be subjective (Buckland and others, 2001). Although we observed evidence of heaping, particularly on the transect line (perpendicular distance=0 m, because of rounding near-line observation angles to 0 degrees), preliminary evaluations using continuous versus binned observation distances (following binning schemes used in prior analyses) found negligible difference in the resulting density estimates and variance. Similar to Peery and others (2006), we evaluated including additional covariates (view conditions, group [cluster] size) that might affect murrelet detectability in preliminary analysis. The addition of these covariates resulted in negligible improvements in model performance (based on AIC) and nearly identical density and variance estimates as models without these covariates (similar to findings of Lorenz and Raphael, 2018).

After-Hatch-Year Abundance Estimates, Trend, and Seasonality

We calculated stratum-specific density estimates for each survey using modeled probability of detection, the number of observed detections per unit length of the transect line (encounter rate), the mean group size of detections, and the length of the transect line. Specifically, the global detection model was applied to annual observation subsets using the "dht2" function in the R "Distance" package (Buckland and others, 2001; Miller and others, 2019). "Distance" averaged results from each survey for each year and multiplied these by the stratum area (104.65 square kilometers [km^2] for each stratum, 209.3 km^2 total) to produce stratum-specific abundance estimates, which were then summed for a total study-area abundance estimate (Buckland and others, 2001; Miller and others, 2019). These design-based abundance estimates simply calculate abundance within the sampled area and extrapolate from this calculation to the study area, assuming sampling effort was allocated randomly (as compared with model-based methods, see "Density Surface Models and Model-Based Abundance Estimates"; Bird and others, 2022).

"Distance" combined variances—reflecting contributions of variance from the mean encounter rate and mean group size each year, and from the detection model—using the delta method, and reported standard errors (SEs) and log-normal 95-percent confidence intervals (CI; Buckland and others, 2001; Miller and others, 2019). We used general linear models (GLMs) to assess potential long-term trends in annual abundance estimates. We evaluated negative binomial and Poisson distribution GLMs and selected the best model using AIC and inspection of residuals. To evaluate the effect of removing flying birds from analysis, we divided annual abundance estimates by the original proportion of birds observed resting on the water and compared the results (appendix 1, fig. 1.2).

To assess the effect and utility of the offshore stratum for estimating AHY abundance and trend throughout the study area, we compared interannual patterns in overall, nearshore, and offshore abundance estimates by computing the *z*-score (annual estimate minus mean of all years, divided by standard deviation) for each geographical grouping. We used a temporal subsetting process to evaluate murrelet densities for seasonality and assess how temporally targeted survey efforts might benefit future survey work. Specifically, using the selected detection function, we generated mean density estimates for 2-week periods throughout the study season, pooling surveys across years in each period. Because sample sizes (number of surveys) varied significantly among 2-week periods and because variance of estimates may be partially related to sample size, we repeated this process using three periods with unequal durations but with similar sample sizes (June 1–July 8, July 9–27, July 28–August 24). We then investigated the effect of reducing sample size (number of annual surveys) by comparing abundance estimates and coefficients of variation (CV) generated for the full study period (June 1–August 24), and two reduced periods (July 1–August 24, and July only); we also compared interannual patterns (as *z*-scores) for the three periods separately. For simplicity and based on nearshore versus offshore results (see "Results"), we performed temporal re-analyses using data from the nearshore stratum only.

Hatch-Year Density Estimates and Productivity Indices

We calculated annual HY density estimates and log-normal 95-percent CIs as described for AHY birds for the nearshore stratum (no HY were seen in the offshore stratum) and for July 10–August 24. This period corresponds to when 34–75 percent of young were expected to fledge and was used by Peery and others (2007) to calculate annual HY:AHY ratios as an index of productivity (for details, see Peery and others, 2007; note that HY murrelets have been detected on surveys as early as June 24; appendix 1, table 1.1). After August 24, AHY birds begin molting to basic (non-breeding winter) plumage, and the two age classes become indistinguishable at sea.

We also calculated annual HY:AHY ratios for the same period following the methods outlined in Peery and others (2007) and Felis and others (2022a): before ratio calculations, we applied date-corrections based on regression models to survey specific HY counts to correct for the expected proportion of unfledged HY birds not yet at sea and AHY counts to correct for the expected number of AHY birds still incubating and not at sea (Peery and others, 2007; Felis and others, 2022a). Full ratio calculation methods are presented in appendix 1 (see "Hatch-Year to After-Hatch-Year Ratio Calculation Methods"). The HY:AHY ratio method assumes all AHY and HY birds observed at sea comprise the local breeding population, but we acknowledge this ratio is sensitive to immigration and emigration of AHY or HY birds. The HY:AHY ratio method also assumes equal detection probability of both age classes among years. To assess whether the interannual pattern of these two measures of reproductive output were similar, especially in light of concerns that occasional immigration of AHY birds from outside the study area might bias results, we compared HY abundance estimates (a productivity index independent of AHY numbers and involving no date corrections) with date-corrected HY:AHY ratios generated using the method of Peery and others (2007) with linear regression.

Density Surface Models and Model-Based Abundance Estimates

We created density surface models (DSMs) to (1) spatially predict murrelet density within the study area, (2) generate maps of long-term and annual density and uncertainty, (3) identify long-term hot spots and annual distributional anomalies, and (4) produce annual model-based abundance estimates. Model-based methods rely on the relationship between species abundance and spatial and environmental covariates to infer abundance in space or time and can relax some assumptions of random sampling required for design-based methods (see "After-Hatch-Year Abundance Estimates, Trend, and Seasonality"; Bird and others, 2022). The "dsm" R package combines detection function models (from the "Distance" package) with generalized additive models (GAMs) for this purpose (Miller and others, 2013, 2019). We segmented GPS survey tracks (when available) or survey routes (when tracks were not available) to approximately 500-m intervals in ArcGIS, and we associated murrelet counts to these segments by spatial proximity and matching date in R. We used distance to coastline and relative alongshore location (from Half Moon Bay to Santa Cruz) as spatial predictor variables. Distance to coastline was calculated using the mainland coast with all offshore rocks excluded except for Año Nuevo Island. Relative alongshore location was calculated as the distance from any location in the study area to a location immediately north of Half Moon Bay. We annotated each segment with the value of each variable based on segment mid-point location (see fig. 1 for distributions of observations and effort with respect to these spatial variables).

For AHY birds, we initially evaluated global negative binomial and Tweedie distribution models with the count of murrelets as a response variable, smooths of the two predictor variables, and segment area as an offset. The negative binomial model had a better initial fit; therefore, we proceeded with evaluating four negative binomial models following Pedersen and others (2019): (1) a global model without year (AHY_dsm_nb); (2) a model with a single common global smoother for all years (AHY_dsm_nb_yrG; Year is a factor random effect and does not interact with the spatial predictor variables); (3) a model with a single common smoother plus group-level (Year) smoothers with the same basis complexity (k, or "wiggliness"; AHY_dsm_nb_yrGS; Year is interacted [as a factor] with each spatial predictor variable); and (4) a model with a single common smoother plus group-level (Year) smoothers with different basis complexities (AHY_dsm_nb_yrGI; Year is included as a random effect and is also interacts as a factor with each spatial predictor variable). We used the default basis complexity (k) for distance to coast (k=10) and a greater value (k=25) for alongshore location to allow greater spatial complexity to fit clustering of murrelets in alongshore hot spots (Bird and others, 2022). To select a final model, we compared all models based on AIC, deviance explained, and evaluated diagnostic plots. We used the final model to predict spatial density and uncertainty (SE and CV) throughout the study area (200–2,500 m from coastline, from Half Moon Bay to Santa Cruz) throughout a 200-m resolution grid for each year; we averaged annual prediction surfaces to calculate a long-term average DSM surface. We generated annual spatial anomaly maps by subtracting the long-term average DSM from each annual DSM; annual DSMs and the long-term average DSM were rescaled (each value divided by respective sum) before subtraction. We also generated annual spatial-model-based abundance estimates and uncertainties for the study area and compared these with design-based results described earlier (see "After-Hatch-Year Abundance Estimates, Trend, and Seasonality").

We used the same spatial predictor variables and settings to generate a negative binomial DSM model for HY murrelets but did not include Year in the model because there were insufficient observations per year (see "Detection Function Modeling"). Therefore, we predicted HY murrelet density across the study area for all years pooled but did not generate annual model-based HY abundance estimates. Finally, we compared predicted spatial distributions of AHY and HY murrelets using a spatial HY:AHY ratio of predicted densities generated by dividing the HY murrelet DSM by the long-term average AHY murrelet DSM.

Results

Detection Functions

Candidate detection function models are compared in table 2. The hazard-rate detection model with Year as a covariate was the best-performing model for AHY murrelets based on AIC (average detectability 0.596 [0.011 SE]; table 2). The Cramér–von Mises goodness-of-fit test was significant at the p=0.05 level for all AHY models, potentially indicating poor fit between models and data. Poor fit seemed to result from rounding ("heaping") of sighting angles to zero for murrelets observed near, but not necessarily on, the survey line (see prominent spike in observation distances at 0-m distance; fig. 2). Because the flat shoulder of the hazard-rate model does not over-fit this spike, and because these observations occurred near the line (within the 20–40-m shoulder of 100-percent detection probability near the vessel; fig. 2), we assumed that the model was appropriate and selected the hazard-rate ~Year model for AHY murrelets.

The hazard-rate model with no covariates and hazard-rate model with Vessel as a covariate had similar AIC values and were selected as top-ranked HY models (table 2). Cramér–von Mises goodness-of-fit tests were not significant at the p=0.05 level for all models, indicating good model fit. We selected the hazard-rate model with Vessel covariate (average detectability 0.508 [0.051 SE]; table 2; fig. 2) for HY murrelets because it had slightly better precision (SE) than the hazard-rate model with no covariates. The results from modeled detection functions for each vessel type were consistent with our expectations, with a greater width of 100-percent detection probability farther from the larger and taller vessel (6-m Whaler or similar, 2007–21) compared with the smaller and lower vessel (4-m Zodiac, 1999–2003; fig. 2). The average probability of detection was greater for AHY murrelets (0.596) compared with HY murrelets (0.508).

After-Hatch-Year Abundance Estimates

Overall and stratum-specific annual AHY murrelet abundance estimates are listed in table 3 and shown on figure 3. The long-term average abundance estimate for the study area was 376 AHY murrelets (range: 163–586 murrelets), and the long-term average CV was 0.176 (range: 0.098–0.297). The long-term average abundance estimate for the nearshore stratum was 350 birds (range: 142–553 murrelets), and the long-term average CV was 0.175 (range: 0.098–0.313). The long-term average abundance estimate for the offshore stratum was 27 murrelets (range: 7–86 murrelets), and the long-term average CV was 0.726 (range: 0.369–1.022).

Examination of the components contributing to the final annual variance (encounter rate, group size, and detection function; table 3) indicated that encounter rate variance was the main positive driver of abundance estimate variance (linear regression slope=0.53, R^2=0.81, p=3.77e−08), and that increased sample size (number of surveys per year) appeared weakly negatively correlated with encounter rate variance (linear regression slope=−0.015, R^2=0.17, p=0.0393; fig. 4). Specifically, estimates from 2001 to 2003 with sample sizes of 12–15 surveys per year had very low and consistent CVs (0.10 each year) compared with other years when 4–9 surveys were performed (CVs 0.12–0.30; table 3).

We selected the negative binomial GLM to estimate the time-series AHY abundance trend because it outperformed the Poisson model (negative binomial AIC=281.1, residual deviance 1.8 on 18 degrees of freedom [df]; Poisson AIC=793.3, residual deviance 635 on 18 df). The negative binomial GLM was not statistically significant at the p=0.05 level, indicating no trend in abundance from 1999 to 2021 (slope=−0.0127, SE=0.00984, t=−1.293, p=0.21). Evaluation of the interannual patterns in abundance estimates (as z-scores) for the study area and nearshore and offshore strata, separately, indicated strong positive correlation between nearshore and total-study-area abundance estimates (linear regression slope=0.986, R^2=0.97, p=2.35e−15; fig. 5). Three outlier years (2007, 2017, 2019) had uncharacteristically greater relative offshore abundances that contributed more to the overall study-area abundance estimates. Nearshore stratum abundance was not significantly related to offshore stratum abundance (linear regression slope=−0.002, R^2=−0.055, p=0.922), and that result was consistent with the exclusion of the three outlier years (fig. 5). A GLM that evaluated abundance estimates for only the nearshore stratum did not indicate a statistically significant interannual trend (slope=−0.01427, SE=0.01039, t=−1.373, p=0.187), which is similar to the result when both strata were combined.

Murrelet density was less in June and August and greater in July, regardless of the temporal grouping scheme (2-week periods with unequal sample sizes or three unequal periods with equal sample sizes; fig. 6). Variance (CVs) were least in July when grouped into 2-week periods, with greater samples sizes having lower CVs (fig. 6). When sample sizes were equivalent in the second grouping scheme, CVs were similar across the full study period (fig. 6). Using data from June 1 to August 24, an average of 7 annual surveys were completed (range: 3–9, excluding 2001–03 when 12–15 surveys completed; table 4). Limiting data to surveys completed from July 1 to August 24 reduced the average to 5 annual surveys (range: 3–8, excluding 2001–03 when 8–12 surveys were completed). During July only, an average of three annual surveys were completed (range: one to five, excluding 2001–03 when seven to nine surveys completed). The average annual abundance estimate (and average CV) was 350 birds (CV: 0.175) for the full study period, 359 birds (CV: 0.188) for July 1–August 24, and 389 birds (CV: 0.179) for July only (table 4). Comparing interannual patterns of abundance (as z-scores) for temporal post-stratifications with the full study period indicated similar results across each temporal grouping (fig. 6), with significant positive correlations between temporal subset estimates and full study period estimates (July 1–August 24 linear regression slope=0.94, R^2=0.87, p=9.64e−10; July 1–31 linear regression slope=0.87, R^2=0.74, p=6.58e−7). The GLMs for annual abundance estimates for July 1–August 24 (slope=−0.90, SE=0.02, t=−1.171, p=−0.257) and July only (slope=−0.006895, SE=0.011126, t=−0.620, p=0.543) did not reveal statistically significant trends, and results were consistent with the result for the full study period.

Table 2. Comparison of detection function models for after-hatch-year (AHY) and hatch-year (HY) Marbled Murrelets (*Brachyramphus marmoratus*) in central California Conservation Zone 6 (Half Moon Bay to Santa Cruz, CA) from 1999 to 2021, during the June 1–August 24 survey season.

[Detection function modeling was limited to murrelets sighted on the water and less than or equal to (≤) 100-meter (m) perpendicular observation distance from the survey transect line. **Abbreviations**: C-vM, Cramér–von Mises goodness-of-fit; SE, standard error; AIC, Akaike information criterion; hr, hazard rate; hn, half-normal; ~, about]

Model	Key function	Formula	C-vM *p*-value	Average detectability (SE)	AIC	Delta AIC
		AHY				
hr_Year[1]	Hazard-rate	~as.factor(Year)	0.015	0.595 (0.011)	−15,895.9	0.0
hn_Year	Half-normal	~as.factor(Year)	0.020	0.560 (0.008)	−15,879.8	16.2
hr	Hazard-rate with cosine adjustment of order 2	~1	0.034	0.559 (0.018)	−15,838.6	57.4
hn	Half-normal with cosine adjustment of order 2,3,4	~1	0.036	0.546 (0.019)	−15,829.0	66.9
		HY				
hr	Hazard-rate	~1	0.827	0.489 (0.052)	−550.6	0
hr_Vessel[1]	Hazard-rate	~Vessel	0.609	0.508 (0.051)	−550.5	0.1
hn	Half-normal with cosine adjustment of order 2,3	~1	0.892	0.475 (0.068)	−549.3	1.3
hn_Vessel	Half-normal	~Vessel	0.488	0.490 (0.032)	−548.7	1.9

[1]Final selected models.

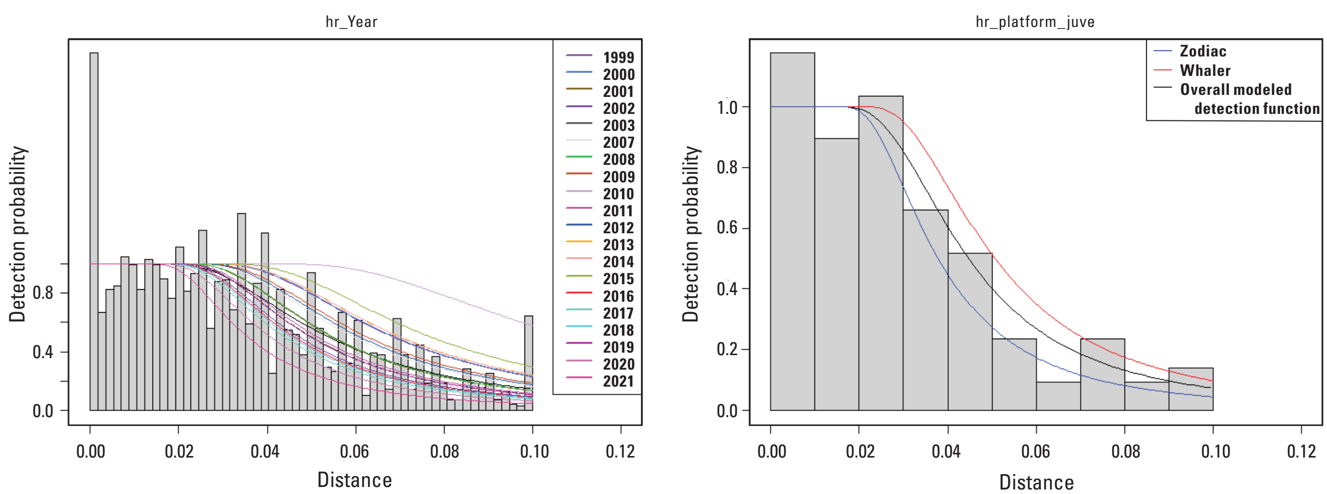

Figure 2. Modeled probability of detection for after-hatch-year (AHY; left) and hatch-year (HY; right). Marbled Murrelets as a function of perpendicular distance (km) from vessel using the top-performing model (hazard rate [hr] with Year as a covariate for AHY; hazard rate with Vessel as a covariate for HY). Histograms show the distribution of observation distances, black line shows the overall modeled detection function, and individually colored lines show the modeled detection function for each level of covariate. Observations were truncated at 100-m (0.1-km) perpendicular distance from the vessel. Note that observation distances were binned for background histogram plotting, but detection-function modeling was done with continuous observation distances.

Table 3. Annual number of surveys, number of Marbled Murrelet detections, mean group size, mean encounter rate (murrelets per kilometer), abundance estimates with log-normal 95-percent confidence interval, and coefficients of variation for all components of abundance estimation for design-based (nearshore stratum, offshore stratum, and total study area) and model-based (total study area) methods.

[k, number of surveys; n, number of Marbled Murrelet detections; CV, coefficient of variation; %, percent; CI, confidence interval, —, not applicable]

k	Stratum	n	Mean group size (CV)	Mean encounter rate (CV)	Detection function (CV)	Design-based abundance		Model-based abundance	
						Abundance estimate (95% CI)	CV	Abundance estimate (95% CI)	CV
1999									
	Nearshore	116	1.72 (0.04)	0.28 (0.11)	0.08	367 (271–496)	0.14	—	—
5	Offshore	2	1.50 (0.33)	0.02 (0.63)	0.08	24 (5–123)	0.72	—	—
	Total	118	1.61 (0.31)	0.23 (0.27)	0.08	391 (290–526)	0.14	370 (264–517)	0.17
2000									
	Nearshore	160	1.79 (0.03)	0.25 (0.17)	0.07	326 (216–494)	0.19	—	—
8	Offshore	2	1.00 (0.00)	0.02 (0.94)	0.07	13 (2–84)	0.94	—	—
	Total	162	1.40 (0.04)	0.21 (0.33)	0.07	339 (226–508)	0.18	337 (261–435)	0.13
2001									
	Nearshore	387	1.85 (0.03)	0.32 (0.08)	0.05	512 (418–628)	0.10	—	—
15	Offshore	7	1.43 (0.21)	0.02 (0.42)	0.05	28 (11–71)	0.47	—	—
	Total	394	1.64 (0.18)	0.26 (0.20)	0.05	540 (442–660)	0.10	510 (424–613)	0.09
2002									
	Nearshore	379	1.79 (0.02)	0.32 (0.08)	0.05	553 (452–676)	0.10	—	—
15	Offshore	3	1.67 (0.20)	0.01 (0.73)	0.05	16 (4–66)	0.75	—	—
	Total	382	1.73 (0.19)	0.25 (0.19)	0.05	569 (465–695)	0.10	470 (388–569)	0.10
2003									
	Nearshore	297	1.82 (0.03)	0.33 (0.08)	0.06	553 (452–675)	0.10	—	—
12	Offshore	6	1.50 (0.15)	0.02 (0.39)	0.06	33 (14–79)	0.43	—	—
	Total	303	1.66 (0.14)	0.26 (0.21)	0.06	586 (481–714)	0.10	600 (493–729)	0.10
2007									
	Nearshore	61	1.70 (0.04)	0.19 (0.16)	0.11	267 (168–424)	0.20	—	—
4	Offshore	4	1.50 (0.19)	0.05 (0.92)	0.11	62 (6–687)	0.95	—	—
	Total	65	1.60 (0.19)	0.16 (0.31)	0.11	329 (190–570)	0.25	304 (216–427)	0.17
2008									
	Nearshore	29	1.72 (0.09)	0.10 (0.23)	0.16	142 (74–274)	0.29	—	—
4	Offshore	1	2.00 (0.00)	0.01 (0.98)	0.16	21 (2–266)	0.99	—	—
	Total	30	1.86 (0.08)	0.08 (0.54)	0.16	163 (87–304)	0.29	126 (87–182)	0.19

Table 3. Annual number of surveys, number of Marbled Murrelet detections, mean group size, mean encounter rate (murrelets per kilometer), abundance estimates with log-normal 95-percent confidence interval, and coefficients of variation for all components of abundance estimation for design-based (nearshore stratum, offshore stratum, and total study area) and model-based (total study area) methods.—Continued

[k, number of surveys; n, number of Marbled Murrelet detections; CV, coefficient of variation; %, percent; CI, confidence interval, —, not applicable]

k	Stratum	n	Mean group size (CV)	Mean encounter rate (CV)	Detection function (CV)	Design-based abundance		Model-based abundance	
						Abundance estimate (95% CI)	CV	Abundance estimate (95% CI)	CV
2009									
8	Nearshore	191	1.74 (0.02)	0.30 (0.12)	0.06	414 (308–557)	0.14	—	—
	Offshore	3	2.00 (0.00)	0.02 (0.54)	0.06	28 (9–93)	0.54	—	—
	Total	194	1.87 (0.02)	0.24 (0.28)	0.06	443 (333–589)	0.13	448 (338–594)	0.14
2010									
7	Nearshore	135	1.66 (0.03)	0.25 (0.17)	0.06	236 (157–356)	0.18	—	—
	Offshore	3	1.67 (0.20)	0.02 (0.66)	0.06	19 (4–83)	0.69	—	—
	Total	138	1.66 (0.20)	0.20 (0.32)	0.06	255 (173–376)	0.18	257 (202–328)	0.12
2011									
6	Nearshore	89	1.63 (0.04)	0.19 (0.05)	0.09	281 (226–349)	0.11	—	—
	Offshore	2	1.50 (0.33)	0.02 (0.62)	0.09	21 (5–102)	0.71	—	—
	Total	91	1.56 (0.32)	0.15 (0.21)	0.09	302 (239–382)	0.12	368 (275–493)	0.15
2012									
6	Nearshore	110	1.77 (0.03)	0.23 (0.13)	0.08	331 (235–468)	0.16	—	—
	Offshore	2	1.50 (0.33)	0.02 (0.64)	0.08	18 (4–89)	0.72	—	—
	Total	112	1.64 (0.31)	0.19 (0.29)	0.08	350 (250–489)	0.15	316 (237–422)	0.15
2013									
6	Nearshore	138	1.70 (0.03)	0.29 (0.21)	0.07	360 (211–614)	0.22	—	—
	Offshore	3	1.67 (0.20)	0.02 (0.71)	0.07	28 (5–142)	0.74	—	—
	Total	141	1.68 (0.20)	0.23 (0.39)	0.07	388 (235–639)	0.22	384 (292–504)	0.14
2014									
9	Nearshore	167	1.82 (0.04)	0.24 (0.17)	0.06	311 (210–461)	0.18	—	—
	Offshore	2	2.50 (0.20)	0.01 (0.68)	0.06	19 (4–80)	0.71	—	—
	Total	169	2.16 (0.23)	0.19 (0.35)	0.06	330 (226–481)	0.18	320 (249–412)	0.13
2015									
9	Nearshore	120	1.77 (0.04)	0.17 (0.15)	0.08	204 (142–294)	0.17	—	—
	Offshore	2	1.00 (0.00)	0.01 (0.68)	0.08	7 (2–29)	0.68	—	—
	Total	122	1.38 (0.05)	0.14 (0.35)	0.08	211 (148–302)	0.17	225 (172–294)	0.14

Table 3. Annual number of surveys, number of Marbled Murrelet detections, mean group size, mean encounter rate (murrelets per kilometer), abundance estimates with log-normal 95-percent confidence interval, and coefficients of variation for all components of abundance estimation for design-based (nearshore stratum, offshore stratum, and total study area) and model-based (total study area) methods.—Continued

[k, number of surveys; n, number of Marbled Murrelet detections; CV, coefficient of variation; %, percent; CI, confidence interval, —, not applicable]

k	Stratum	n	Mean group size (CV)	Mean encounter rate (CV)	Detection function (CV)	Design-based abundance		Model-based abundance	
						Abundance estimate (95% CI)	CV	Abundance estimate (95% CI)	CV
2016									
7	Nearshore	153	1.90 (0.03)	0.28 (0.19)	0.08	523 (328–833)	0.21	—	—
	Offshore	1	1.00 (0.00)	0.01 (1.01)	0.08	7 (1–51)	1.01	—	—
	Total	154	1.45 (0.04)	0.22 (0.45)	0.08	529 (334–839)	0.20	591 (433–805)	0.16
2017									
9	Nearshore	153	1.69 (0.04)	0.21 (0.13)	0.07	374 (272–516)	0.15	—	—
	Offshore	10	1.60 (0.14)	0.05 (0.33)	0.07	86 (39–187)	0.37	—	—
	Total	163	1.64 (0.14)	0.18 (0.27)	0.07	460 (341–620)	0.15	437 (339–564)	0.13
2018									
9	Nearshore	109	1.65 (0.03)	0.15 (0.16)	0.08	255 (171–378)	0.19	—	—
	Offshore	2	1.00 (0.00)	0.01 (0.65)	0.08	10 (3–41)	0.66	—	—
	Total	111	1.33 (0.04)	0.12 (0.31)	0.08	265 (180–389)	0.18	257 (198–334)	0.13
2019									
8	Nearshore	103	1.74 (0.04)	0.16 (0.17)	0.09	265 (175–402)	0.19	—	—
	Offshore	5	2.00 (0.27)	0.03 (0.57)	0.09	55 (15–200)	0.64	—	—
	Total	108	1.87 (0.30)	0.13 (0.29)	0.09	320 (213–480)	0.20	310 (228–421)	0.16
2020									
9	Nearshore	153	1.70 (0.03)	0.21 (0.16)	0.07	394 (268–580)	0.18	—	—
	Offshore	1	2.00 (0.00)	0.01 (1.02)	0.07	12 (2–83)	1.02	—	—
	Total	154	1.85 (0.03)	0.17 (0.32)	0.07	406 (278–593)	0.18	438 (321–597)	0.16
2021									
9	Nearshore	105	1.79 (0.03)	0.15 (0.30)	0.09	322 (163–638)	0.31	—	—
	Offshore	3	1.33 (0.25)	0.02 (0.71)	0.09	27 (6–121)	0.76	—	—
	Total	108	1.56 (0.22)	0.12 (0.54)	0.09	349 (184–662)	0.30	348 (259–467)	0.15

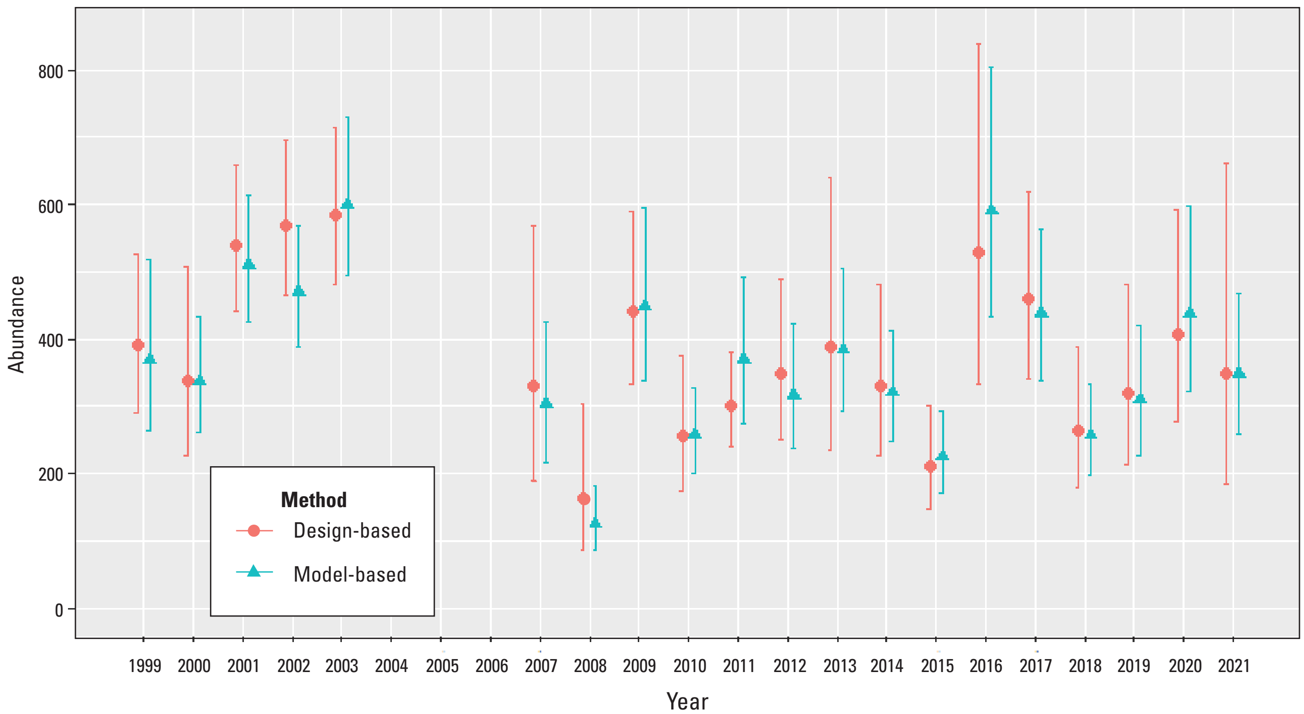

Figure 3. Design- and model-based annual Marbled Murrelet abundance estimates and log-normal 95-percent confidence limits (error bars) for the study area (combined nearshore and offshore strata) for all surveys June 1–August 24.

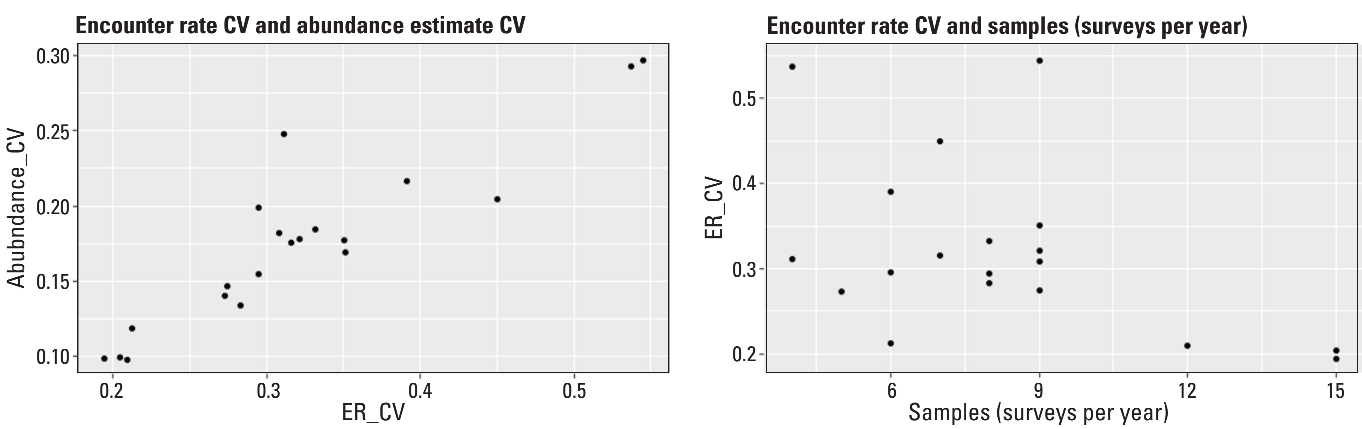

Figure 4. Left: Comparison of annual design-based abundance estimate coefficients of variation (CV) and encounter rate (ER) CVs. Right: Comparison of annual ER CVs and sample sizes (surveys per year).

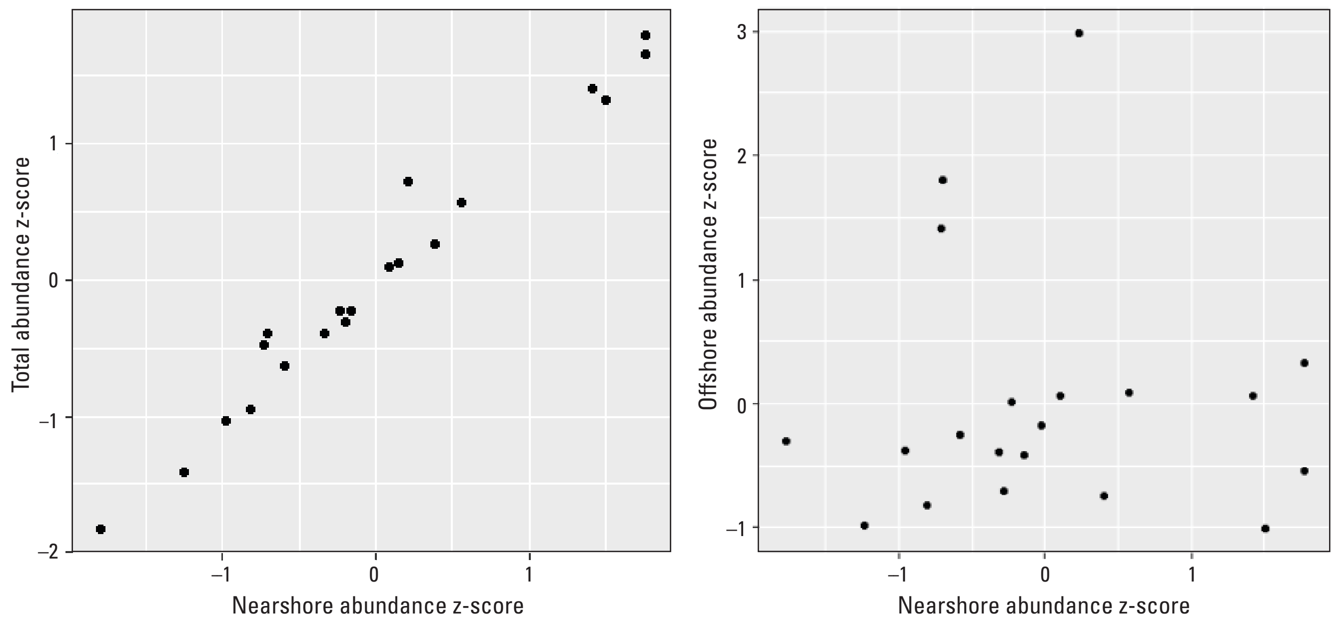

Figure 5. Left: Comparison of total (nearshore and offshore strata combined) Marbled Murrelet annual abundance estimate *z*-scores and nearshore-only abundance estimate *z*-scores. Right: Comparison of offshore-only abundance estimate *z*-scores and nearshore-only abundance estimate *z*-scores.

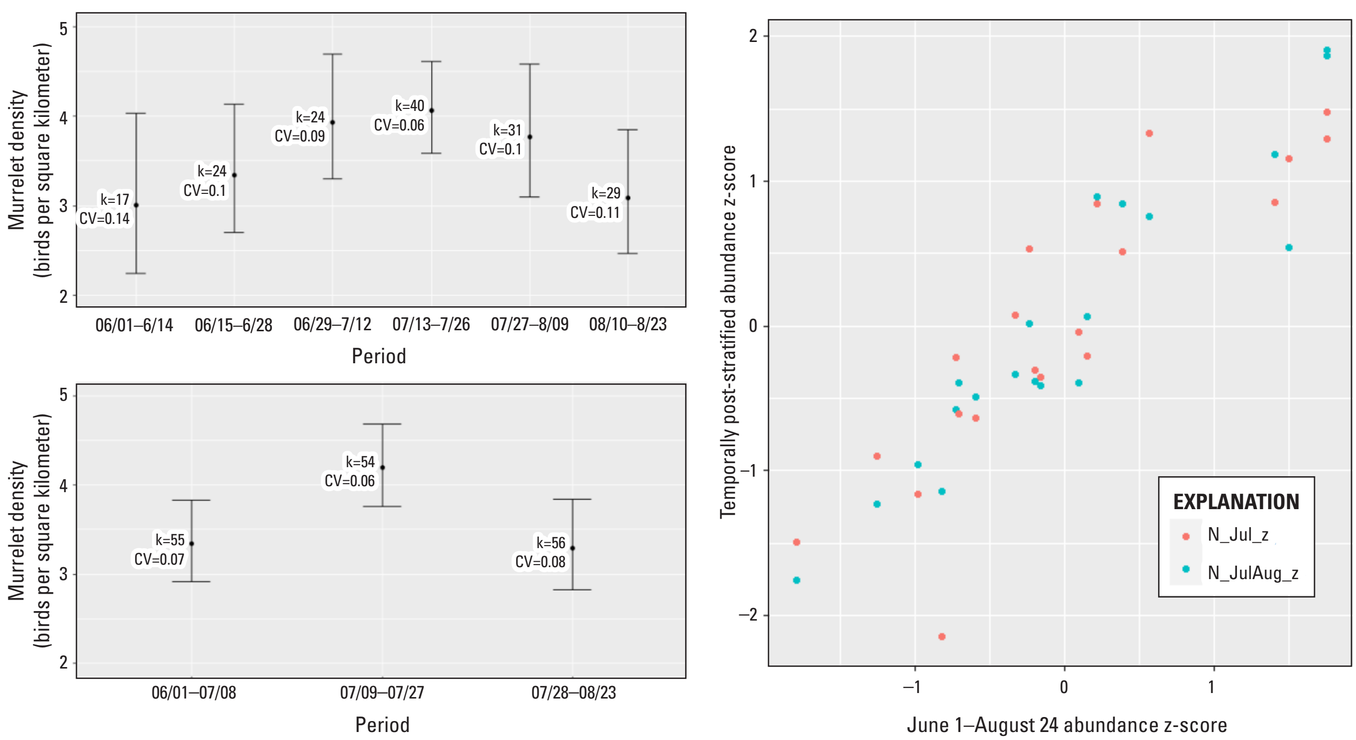

Figure 6. Estimated long-term (1999–2021) Marbled Murrelet densities (±95-percent confidence interval error bars) for 2-week periods with unequal sample sizes (top left panel) and three unequal periods with equivalent sample sizes (bottom left panel) for all years pooled. Sample size (k, number of surveys) and coefficient of variation (CV) are labelled beside each point. Right panel shows temporally post-stratified abundance estimate *z*-score values (July-only, and July 1–August 24) compared with full study period abundance estimate *z*-score values (June 1–August 24).

Table 4. Temporal post-stratification results for annual Marbled Murrelet design-based abundance estimates indicating sample size, abundance estimate, and abundance estimate coefficient of variation for the full study period (June 1–August 24), July 1–August 24, and July only.

[Results are for the nearshore stratum only. **Abbreviations**: k, number of surveys; N, number of murrelets; CV, coefficient of variation]

Year	June 1–August 24			July 1–August 24			July 1–July 31		
	k	N	CV	k	N	CV	k	N	CV
1999	5	367	0.140	5	367	0.140	4	362	0.158
2000	8	326	0.187	5	311	0.218	3	349	0.163
2001	15	512	0.100	12	506	0.106	9	498	0.135
2002	15	553	0.098	12	590	0.098	8	554	0.123
2003	12	553	0.098	8	596	0.122	7	579	0.137
2007	4	267	0.198	3	310	0.166	3	310	0.166
2008	4	142	0.291	4	142	0.291	2	197	0.229
2009	8	414	0.136	5	453	0.189	3	559	0.185
2010	7	236	0.179	4	240	0.151	4	240	0.151
2011	6	280	0.110	4	299	0.102	2	307	0.108
2012	6	331	0.156	4	308	0.217	3	344	0.207
2013	6	360	0.225	4	311	0.281	3	383	0.233
2014	9	311	0.181	8	318	0.200	5	399	0.200
2015	9	204	0.172	7	207	0.213	4	273	0.185
2016	7	522	0.206	6	426	0.174	3	537	0.222
2017	9	374	0.151	6	469	0.133	4	497	0.150
2018	9	254	0.186	7	217	0.214	1	113	0.171
2019	8	265	0.193	6	287	0.206	2	360	0.163
2020	9	394	0.179	6	463	0.174	3	454	0.142
2021	9	322	0.313	7	361	0.362	5	457	0.359

Hatch-Year Abundance Estimates and Productivity Indices

Annual HY Marbled Murrelet abundance estimates and date-corrected HY:AHY ratios are listed in table 5 and shown in figure 7. The long-term average HY abundance estimate was 13 birds (range: 0–31 annually), and the long-term average CV was 0.57 (range: 0.25–1.00 annually). The long-term average HY:AHY ratio was 0.052 (range: 0.00–0.12), and the long-term average CV was 0.52 (range: 0.18–1.06; table 5). The HY:AHY ratios and HY abundance estimates were positively correlated (linear regression slope=253.9, R^2=0.81, p=7.85e−8; fig. 7), and average CVs were similar (0.57 and 0.52, respectively). Neither the HY abundance estimates or the HY:AHY ratios indicated evidence of trend throughout time (HY abundance negative binomial GLM slope=−0.02825, SE=0.02281, t=−1.238, p=0.231; HY:AHY ratio negative binomial GLM slope=−0.001, SE=0.0202, t=−0.048, p=0.962).

Density Surface Models

The GAM for AHY murrelets that allowed modeled responses to vary most by year (AHY_dsm_nb_yrGI) performed best based on AIC and greatest deviance explained (40 percent; table 6). This model also indicated good diagnostic results based on inspection of residual quantile-quantile plots (see appendix 1, section "Density Surface Model Diagnostics and Additional Results", fig. 1.4). Overall responses of counts to the two predictor variables are shown in figure 8 (see appendix 1, section "Density Surface Model Diagnostics and Additional Results" for annual response plots [fig. 1.3] and significance terms). Murrelet counts were predicted to be greatest nearshore and least offshore (fig. 8). With respect to alongshore location, predicted counts were greatest within the central study area, moderate within the north, and least within the south (with the exception of waters near Santa Cruz; fig. 8).

Year was significant as a random effect in the model ($p<2e-16$) and year-specific responses to alongshore location were nearly always significant, indicating annual variability in alongshore distribution (see appendix 1, section "Density Surface Model Diagnostics and Additional Results"). In contrast, relatively few year-specific responses to distance to coast were significant, indicating less annual variability (see appendix 1, section "Density Surface Model Diagnostics and Additional Results"). The spatial average of annual DSM predictions is shown in figure 9, and annual spatial anomalies are shown in appendix 1, figure 1.5. Comparison of AHY abundance estimates and CVs for the traditional design-based method and for DSM model-based method are shown in table 3 and figure 3. The long-term average model-based abundance estimate was 371 murrelets (range: 126–600), and the long-term average CV was 0.14 (range: 0.09–0.19; table 3).

The GAM model for HY murrelets explained 27 percent of the deviance in HY counts (see appendix 1, section "Density Surface Model Diagnostics and Additional Results" for model diagnostics, fig. 1.6). Responses of counts to the two predictor variables are shown in figure 8, and the DSM prediction map is shown in figure 10. The HY model indicated generally similar responses to the predictor variables compared with the AHY model, although with a steeper nearshore-offshore gradient in predicted counts (compare magnitude of response [*y*] axes in fig. 8) and subtle differences in alongshore location (fig. 8). The HY murrelets were predicted to be greatest within the central study area, low to moderate to the north, and mostly absent in the south (fig. 10). The spatial HY:AHY ratio highlighted nearshore waters between Point Año Nuevo and Scott Creek as having the greatest HY densities relative to AHY murrelets in the study area (fig. 10).

Table 5. Annual hatch-year (HY) Marbled Murrelet abundance estimates and hatch-year:after-hatch-year (HY:AHY) ratios, including log-normal 95-percent confidence intervals, standard errors, coefficients of variation, sample size, and number of HY murrelet detections for all surveys performed July 10–August 24.

[Note that number of detections (n) is specific to abundance estimation wherein observations beyond 100 meters from the vessel were removed for distance analysis, whereas the HY:AHY ratio method used all HY and AHY observations regardless of observation distance (see table 1 for annual age-class totals and appendix 1, table 1.1 for survey-specific age class totals). **Abbreviations**: k, number of surveys; %, percent; CI, confidence intervals; SE, standard errors; CV, coefficients of variation; NA, not applicable]

Year	k	Abundance				HY:AHY Ratio		
		n	Estimate (95% CI)	SE	CV	Estimate (95%CI)	SE	CV
1999	4	5	18 (4–97)	11.2	0.60	0.057 (0.024–0.138)	0.027	0.47
2000	4	2	7 (1–38)	4.3	0.61	0.024 (0.010–0.061)	0.012	0.50
2001	8	13	23 (12–43)	6.9	0.30	0.070 (0.039–0.124)	0.021	0.30
2002	11	15	20 (12–34)	5.1	0.25	0.051 (0.036–0.072)	0.009	0.18
2003	8	10	19 (11–35)	5.6	0.29	0.049 (0.032–0.076)	0.011	0.22
2007	3	2	8 (0–247)	7.9	0.97	0.049 (0.009–0.269)	0.052	1.06
2008	4	0	0	NA	NA	0	NA	NA
2009	4	3	9 (1–54)	5.7	0.64	0.028 (0.009–0.089)	0.018	0.64
2010	3	4	16 (2–116)	8.5	0.53	0.081 (0.033–0.198)	0.039	0.48
2011	3	5	19 (4–83)	7.9	0.41	0.080 (0.052–0.124)	0.018	0.23
2012	3	1	5 (0–136)	4.6	0.94	0.029 (0.008–0.109)	0.022	0.76
2013	3	8	31 (6–175)	14.7	0.47	0.122 (0.048–0.312)	0.062	0.51
2014	6	12	24 (7–84)	12.7	0.54	0.081 (0.036–0.182)	0.035	0.43
2015	6	4	8 (3–17)	2.6	0.34	0.059 (0.031–0.113)	0.020	0.34
2016	5	11	26 (8–81)	11.7	0.45	0.108 (0.045–0.260)	0.051	0.47
2017	6	3	6 (1–28)	4.0	0.69	0.022 (0.007–0.074)	0.015	0.68
2018	6	4	8 (2–35)	5.1	0.65	0.047 (0.014–0.158)	0.032	0.68
2019	6	3	6 (1–29)	4.1	0.69	0.025 (0.006–0.099)	0.020	0.80
2020	6	2	4 (0–32)	3.9	1.00	0.018 (0.006–0.054)	0.011	0.61
2021	6	4	8 (2–25)	3.9	0.50	0.041 (0.014–0.119)	0.024	0.59

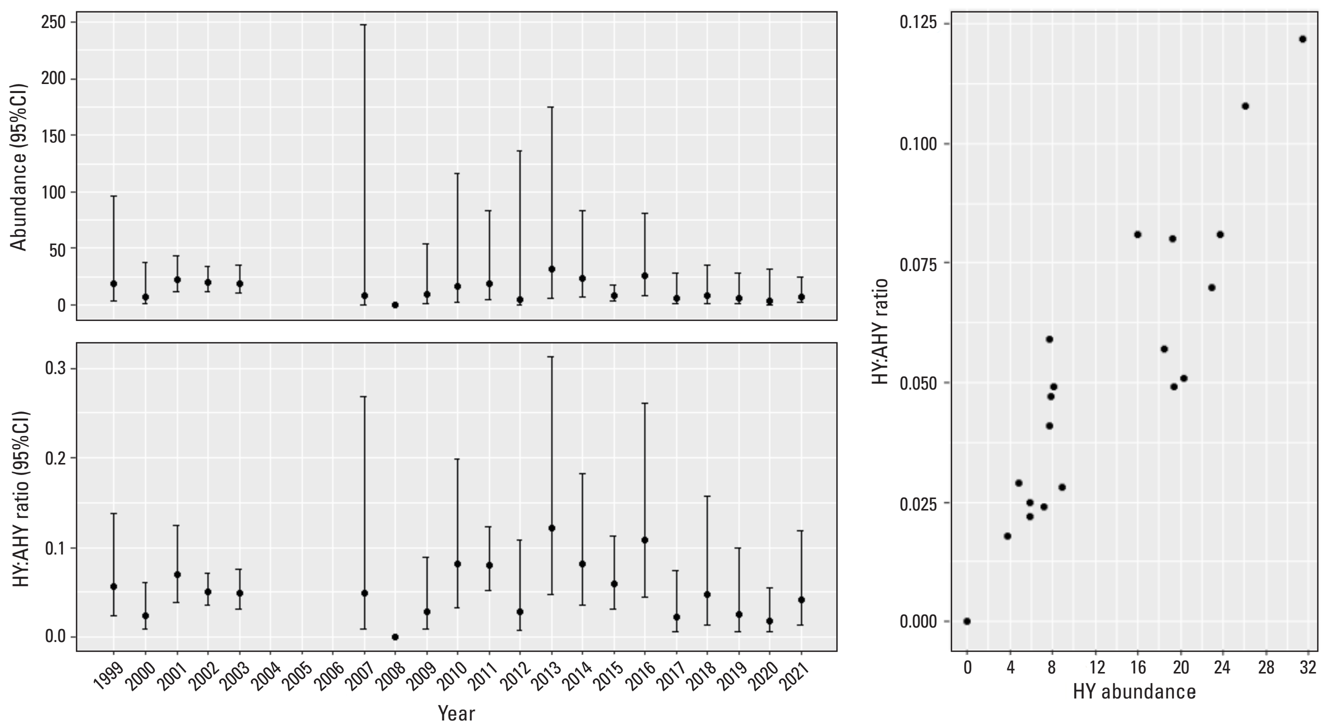

Figure 7. Top left plot: Annual hatch-year (HY) Marbled Murrelet abundance estimates with log-normal 95-percent confidence intervals (CI). Bottom left plot: Annual Marbled Murrelet date-corrected hatch-year:after-hatch-year (HY:AHY) ratios with log-normal 95-percent confidence intervals (CI). Right plot: Comparison of annual HY:AHY ratios to HY abundance estimates.

Table 6. Density surface model selection for after-hatch-year (AHY) Marbled Murrelets.

[R^2, R-squared; AIC, Akaike information criterion]

Model name	Family	Formula	R^2 adjusted	Percent deviance explained	Delta AIC
AHY_dsm_nb_yrGI	Negative Binomial (0.107)	count ~ s(mamu_along, k=25) + s(dstcstmain, k=10) + s(mamu_along, by = Year, m=1, k=25) + s(dstcstmain, by = Year, m=1, k=10) + s(Year, bs = "re", k=20) + offset(seg.area)	0.092	39.9	0
AHY_dsm_nb_yrGS	Negative Binomial (0.096)	count ~ s(mamu_along, k=25) + s(dstcstmain, k=10) + s(mamu_along, Year, bs = "fs", k=25) + s(dstcstmain, Year, bs = "fs", k=10) + offset(seg.area)	0.066	35.4	159.4
AHY_dsm_nb_yrG	Negative Binomial (0.089)	count ~ s(mamu_along, k=25) + s(dstcstmain, k=10) + s(Year, k=20), bs = "re") + offset(seg.area)	0.054	32.0	362.1
AHY_dsm_nb	Negative Binomial (0.085)	count ~ s(mamu_along, k=25) + s(dstcstmain, k=10) + offset(seg.area)	0.053	30.4	474.3

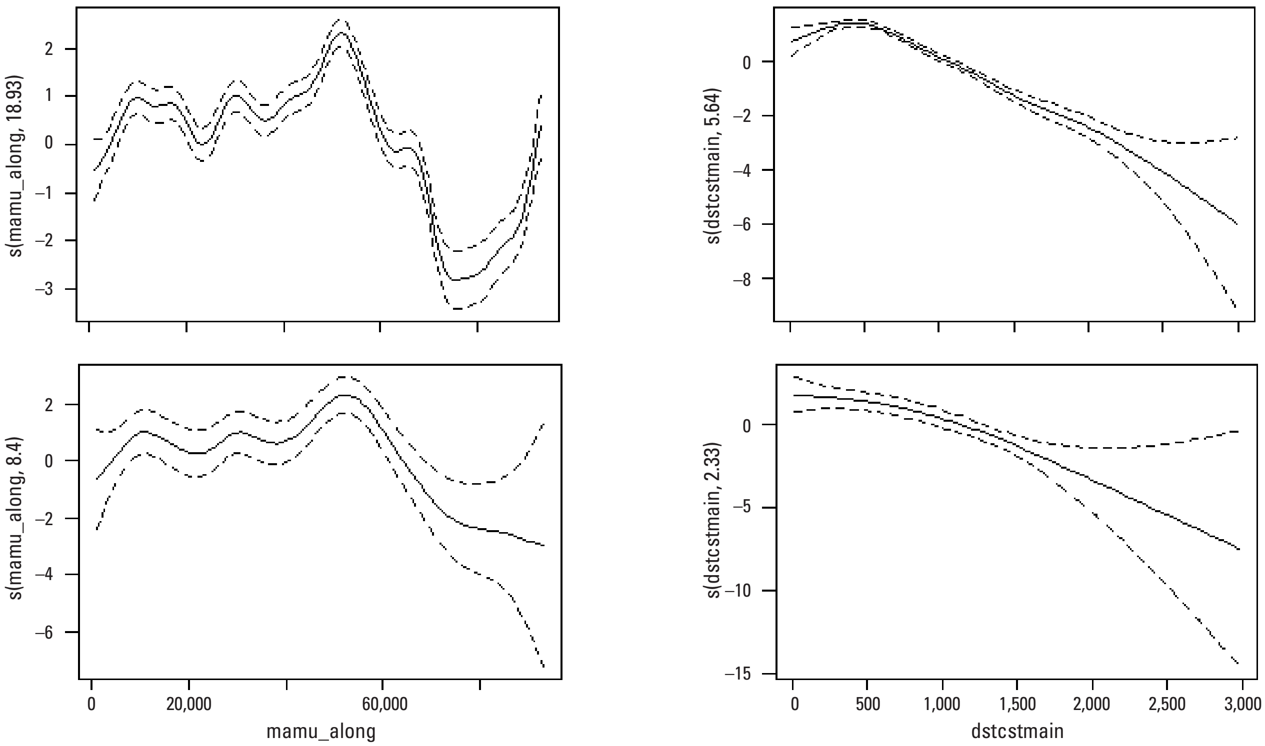

Figure 8. Response plots of spatial smooths of alongshore position (left) and distance to coast (in meters; right) from generalized additive model (GAM) density surface model of Marbled Murrelet counts for after-hatch-year (AHY) murrelets (top row) and hatch-year (HY) murrelets (bottom row). Alongshore position was quantified from Half Moon Bay (0 meters; left side of *x*-axis) to Santa Cruz (about 90,000 meters, right side of *x*-axis).

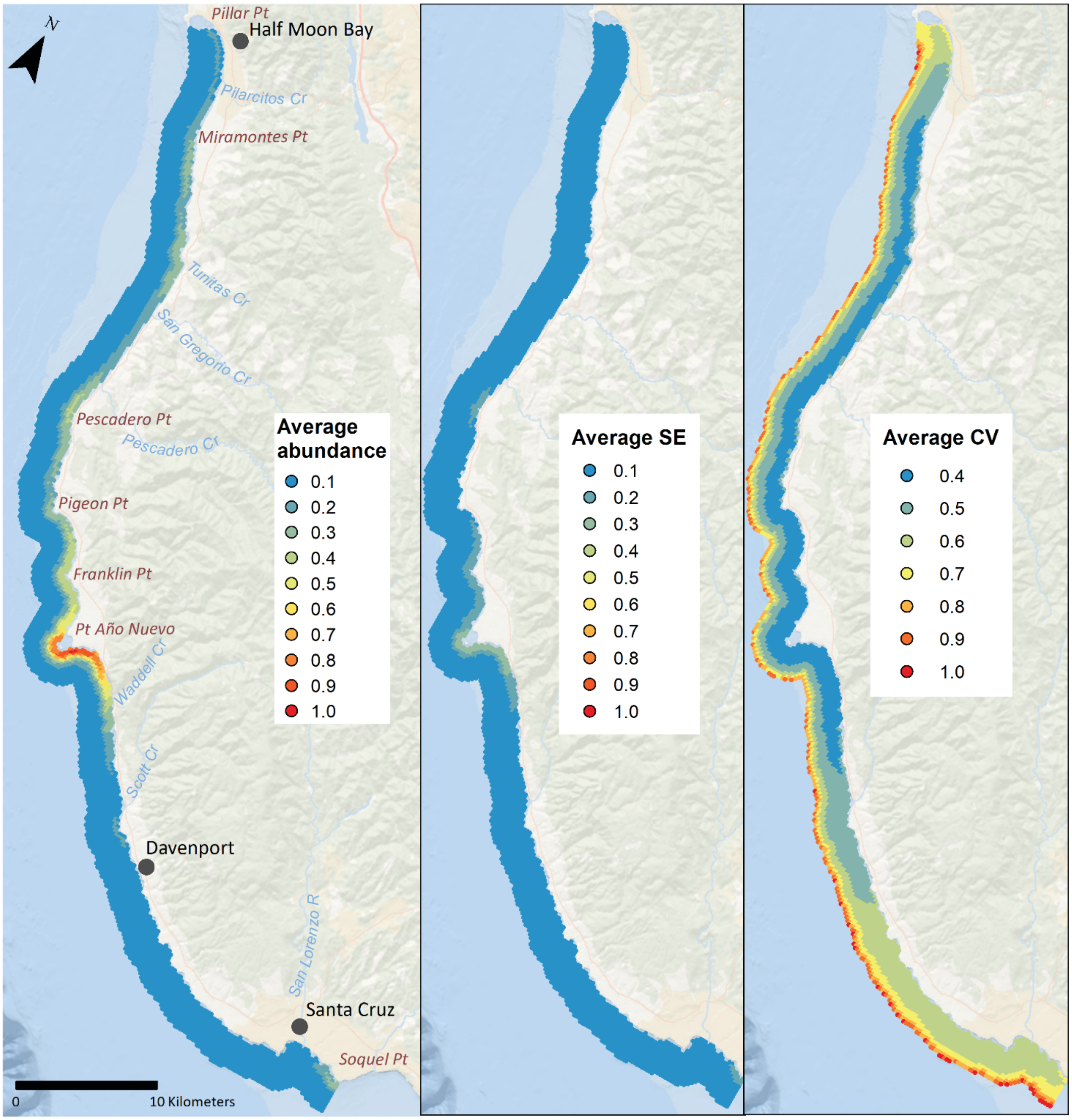

Base map from Esri and its licensors, copyright 2022

Figure 9. Long-term average of annual density surface model predictions of AHY Marbled Murrelet abundance (number of birds in 200-m grid cells; left panel), abundance standard error (middle panel), and CV (right panel).

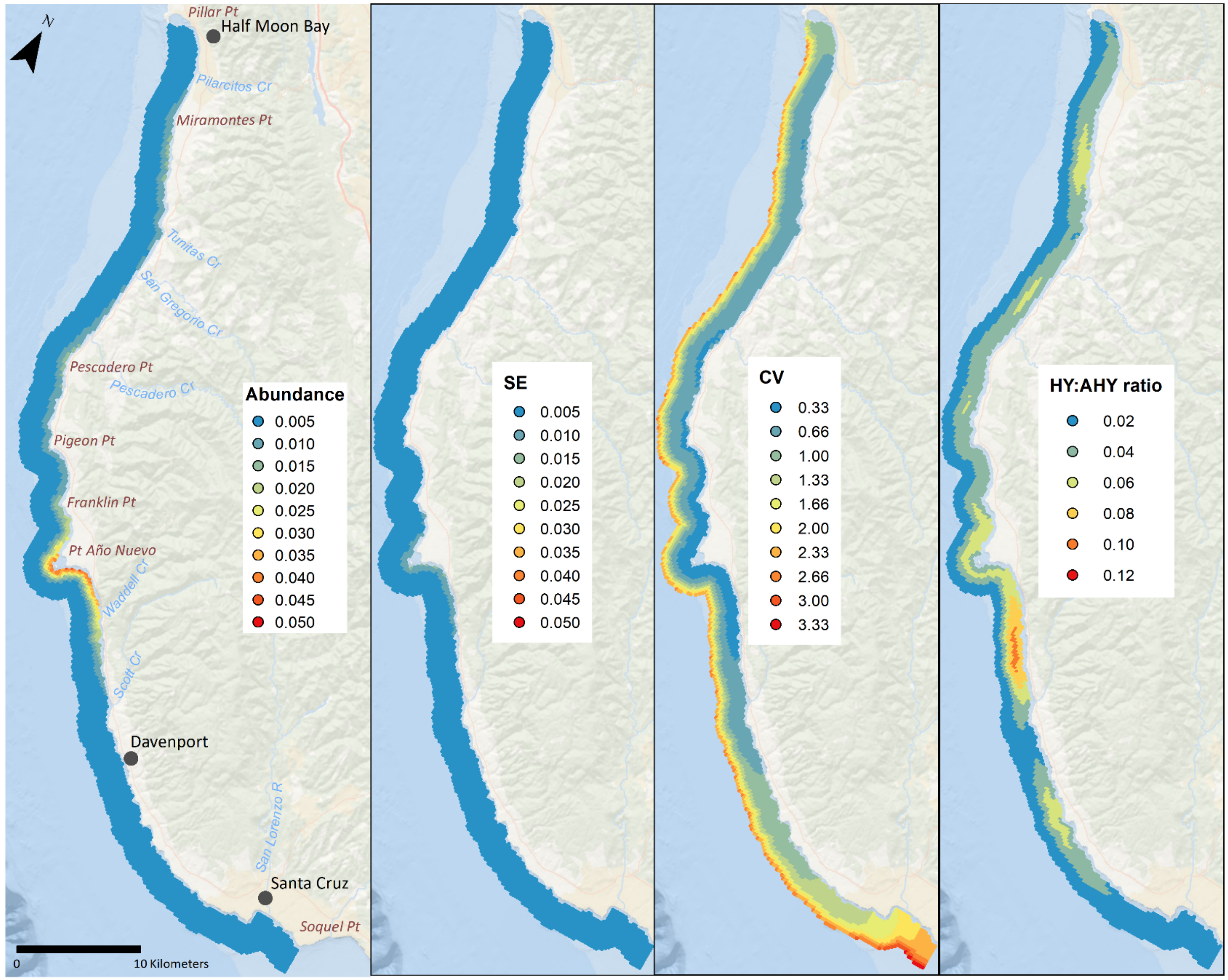

Base map from Esri and its licensors, copyright 2022

Figure 10. Density surface model predictions of HY Marbled Murrelet abundance (number of birds in 200-m grid cells), abundance standard error (SE), coefficient of variation (CV), and spatially explicit hatch-year (HY) to after-hatch-year (AHY) ratio generated by dividing the HY murrelet density surface model (DSM) by the long-term average AHY murrelet DSM.

Discussion

After-Hatch-Year Murrelet Abundance, Distribution, and Monitoring

We updated annual at-sea abundance estimates for Marbled Murrelets in central California Conservation Zone 6 using comprehensive and consistent analytical methods for a 23-year time series (1999–2021). The long-term average, design-based AHY abundance estimate for the study area was 376 murrelets (range: 163–586 murrelets; table 3). Our results indicated similar interannual patterns, but indicated slightly fewer murrelets overall, than those reported previously using less consistent methods annually (long-term average 485 murrelets, range: 174–699 murrelets annually; see Felis and others [2022a]). Lesser abundances may have resulted from the exclusion of flying birds in our analysis, which were inconsistently recorded throughout time, but also likely resulted from the change in detection function model from a half-normal function in previous analyses to a hazard rate key function. Our global hazard rate detection function model with Year as a covariate was the best fit for these data; this model also had a greater detection probability (table 2), resulting in slightly lesser overall abundance estimates than past half-normal model estimates. Although the removal of flying murrelets did not drastically change interannual patterns in abundance estimates (appendix 1, fig. 1.2), they could be reincorporated into analysis with the caveat that it would limit retrospective comparison to about 2010–present when flying murrelets were consistently recorded. Our new analytical approach using an annually varying global detection model will result in minor updates to past annual estimates every year; however, pooling more observations across years increases the robustness and accuracy of the model results. Re-evaluation of model specifics, such as key function and covariates, could be done on longer time-spans (for example, every 5 years).

After-hatch-year murrelets were predominantly concentrated in the nearshore stratum (200–1,350 m from shore; fig. 1; table 3), which was mostly less than 800 m from shore (figs. 8, 9), consistent with results from exploratory surveys during the 1990s that affected the sampling design of this monitoring program (Becker and others, 1997; see appendix 1, section "Density Surface Model Diagnostics and Additional Results"). With respect to alongshore location, the distribution of murrelets was more clumped overall (figs. 1, 8, 9) and more annually variable than distribution associated with distance to coast (see annual spatial distribution anomaly maps, see appendix 1, section "Density Surface Model Diagnostics and Additional Results"). Based on telemetry (Peery and others, 2009) and at-sea survey data (Becker and Beissinger, 2003), murrelets in this study area were more clumped in waters near nesting areas (for example, Año Nuevo Bay near old-growth forests in Big Basin State Park) during periods with greater upwelling (and presumably better foraging conditions) compared to oceanic relaxation periods.

Of the three sources of uncertainty in the design-based abundance estimates (encounter rate, group size, and detection model), the variance in murrelet encounter rate across surveys was the primary driver of uncertainty, resulting in annual CVs of 0.10–0.30 (table 3). Sample size (number of surveys per year) was weakly, negatively correlated with encounter rate CV; sample sizes of 12–15 surveys per year (2001–03) resulted in consistently low CVs (0.10) compared with samples sizes of 9 or less (all other years), which had more variable and often greater CVs. For years with nine or fewer surveys, sample size reduction (because of temporal subsetting) indicated little change in average annual CV or in interannual patterns and trend in abundance estimates, indicating little difference in results when surveying an average of three, five, or seven times per year; however, significant improvements in uncertainty were gained by surveying 12–15 times per year.

The long-term AHY murrelet abundance at sea in Zone 6 seemed stable, and we did not detect any statistically significant trend for 23 years. Based on a simulation of 10 surveys per year for 10 years with our study design and simulated murrelet densities/distributions generated from preliminary surveys in our study area, Rachowicz and others (2006) estimated a 90-percent power to detect a 4 percent decline in at-sea abundance per year with CVs of 0.13–0.17 (the upper limit of which is similar to the average CV in our results). Although we did not do a new power analysis, we expect similar power to detect a similar rate of decline.

Murrelet densities were greatest in July and least in June and August, which is consistent with initial exploratory surveys (Becker and others, 1997). Variance was similar among these different temporal subsets of the season (when sample size was held constant), indicating that focusing survey effort during any one part of the season might not reduce variability in annual abundance estimates compared to any other part of the season, although a shorter-duration survey window could be logistically beneficial and still retain the ability to compare with past years. However, fewer surveys in narrower time windows resulted in abundance estimate CVs similar to full-season estimates with more surveys, indicating that a reduction in sample size is offset by more consistency in surveys performed in a narrower time window. The seasonal changes in murrelet densities in our study, which was also observed by Becker and others (1997), could be driven in part by nesting phenology. Birds incubating eggs in June are absent from the water, resulting in lower at-sea densities, followed by an increase in at-sea density during chick-provisioning in July when most locally breeding murrelets are on the water except for short provisioning trips in the early morning and early evening hours. Finally, murrelet density might decrease again in August post-breeding when some individuals disperse out of the study area. Immigration or emigration of murrelets from or to other areas could also contribute to the observed patterns. However, Peery and others (2008) detected only 7 percent of radio-marked murrelets dispersed southward out of our study area during the breeding season, and genetic studies indicated only 6 percent of central California murrelets likely were immigrants during the breeding season (Hall and others, 2009).

Model-based abundance estimates (long-term annual average 371 murrelets, range: 126–600) were similar to design-based estimates for most years, but uncertainty (as expressed by CV) typically was less using the model-based method, especially during years with greatest CVs using the design-based method (table 3). Design-based methods assume a uniform distribution of individuals in relation to transects to ensure unbiased inference to the sample population of interest; however, the randomized design of transects can sometimes be difficult to implement in the field (Schmidt and Deacy, 2021). In our case, sampling effort was designed to be uniform with respect to alongshore location and distance to coastline within each stratum; *post hoc* inspection of effort indicated this assumption generally was met with respect to alongshore location (although see below on transect draw direction); however, survey effort was slightly biased toward the nearshore in each stratum (fig. 1), potentially biasing abundance estimates upward because of the prevalence of murrelets close to shore. In addition, it was discovered during previous years that survey routes created when using the southern end of the survey area as the starting point resulted in a greater likelihood of encountering high-density murrelet areas (for example, Año Nuevo Bay) due to the complex coastline geometry. This likelihood could potentially affect the encounter rate depending on how the survey transect was created and increase variance annually for design-based estimates. Spatial models of density and abundance relax some of the assumptions needed for unbiased, design-based estimates because spatial relationships of animal observations and habitat features are explicitly modeled (Schmidt and Deacy, 2021). In our case, using a model-based design reduced the CVs associated with abundance estimates, and this method could be used in future analyses. We created simple spatial models to predict murrelet density that did not include ecologically explanatory habitat variables; although these models are not directly transferable to other regions for prediction purposes, they do provide reasonable spatial predictions and estimates with reduced variances for the Zone 6 study area.

The overall interannual pattern in abundance estimates (and CVs; table 3) was almost entirely driven by results from the nearshore stratum, as expected. Although CVs for the offshore stratum were greater than in the nearshore, offshore results contributed little to overall annual abundance estimates and only moderately to CVs because so few birds were seen offshore (7 percent of the long-term average abundance estimate was from the offshore stratum; table 3). We suggest that the existing nearshore-offshore effort stratification is valid as designed given the distribution of murrelets in the study area, but the offshore stratum need not be surveyed, especially given how invariable murrelet density is with respect to distance from coast among years. Incorporating the offshore stratum into abundance estimation provided a more complete overall estimate of abundance for the region but did not affect our ability to detect change in abundance over time. Meanwhile, nearshore-offshore distribution did not vary much annually based on our model-based results, similar to long-term findings of the other five Conservation Zones (McIver and others, 2021). Years with low abundance (for example, 2008) have been associated with temporary dispersal out of the study area (Peery and others, 2006; Vásquez-Carrillo and others, 2013) and not with greater offshore abundance in the study area. More importantly, significant interannual differences in alongshore murrelet density (fig. 1), combined with the fact that north-drawn transects tend to miss alongshore hotspots with greater murrelet densities compared with south-drawn transects, indicates that increasing survey effort in the nearshore stratum would generate more precise annual estimates with reduced variance. For example, existing offshore survey effort could be reallocated to the nearshore stratum (with a tighter zig-zag design) to more effectively survey persistent, alongshore murrelet hotspots. Using model-based analytical methods could also improve estimates, as discussed earlier.

The logistics of surveying this study area are dictated primarily by weather conditions. Increasing late morning–afternoon winds deteriorate observation conditions below acceptable levels, limiting survey timing to the first half of the day, equivalent to the shortest period that the 100-km effort can be accomplished. Maintaining effort in the offshore stratum while simultaneously increasing effort in the nearshore would not be feasible. Increasing the number of surveys to 12–15 or more per season could reduce variability in abundance estimates; however, reducing the number of surveys per season to fewer than 10 would not significantly change abundance estimates nor ability to detect trends and maintains sufficient effort to compare with past years. Given that most historical effort has occurred in July and August and that surveys closer in time result in density estimates that are more similar (Becker and others, 1997), increased spatial effort in just the nearshore stratum during a more limited period (such as the density "peak" in late June–early August) and using model-based estimation methods may provide the best logistical and analytical benefits in the future while maintaining ability to compare future results with past years. On the other hand, focusing survey effort in June potentially could be a better measure of the local breeding population, assuming more birds immigrate to Zone 6 as the season progresses and would also be more consistent with the timing of surveys in Zones 1–5 (McIver and others, 2021).

Hatch-Year Murrelet Abundance, Distribution, and Monitoring

We estimated annual HY murrelet abundance incorporating detection-function-modeling for the first time in Zone 6 to evaluate local reproductive output independent of AHY murrelet abundance at sea. Reproductive output has traditionally been reported as the ratio of HY:AHY birds without detection function modeling, but with date-corrections to account for the expected proportions of adults still incubating and juveniles not yet fledged (Peery and others, 2007; Felis and others, 2022a). The long-term average HY abundance estimate was 13 murrelets (range: 0–31 birds annually), equating to a long-term abundance-estimate-based HY:AHY ratio of 0.035. By comparison, the long-term average HY:AHY ratio calculated with traditional methods (based on encounter rates and phenological date corrections; appendix 1) was 0.052, which is similar to results using comparable methods in Washington (mean: 0.07, range: 0.02–0.12; Lorenz and Raphael, 2018) where far greater numbers of murrelets exist. Both metrics were positively correlated, indicating that each provided similar information annually. Despite significant interannual variability in each metric, neither indicated a statistically significant trend throughout time. The average probability of detection seemed greater for AHY birds (0.596) compared with HY birds (0.508), consistent with field observations (HY birds tend to do more evasive diving and may be harder to detect). This discrepancy in detectability could bias HY:AHY ratio estimates (based on raw counts that are not distance-corrected) to be lesser. However, the inclusion of hypothetical unfledged HY birds (based on date) into HY:AHY ratios would increase the HY:AHY ratio and probably more than offset the effect of difference in detection probability between the two age classes.

Variance associated with HY abundance estimates (annual CV range: 0.25–1.00) was greater than that of AHY abundance estimates (annual CV range: 0.01–0.30), and HY:AHY ratio variance was also high (annual CV range: 0.18–1.06), probably owing to fewer annual surveys (limited to the HY time window), very low numbers of HY sightings, and greater variability in encounter rates. There was large overlap among interannual HY abundance estimates and HY:AHY ratios at the 95-percent CI level, making it difficult to evaluate interannual differences. The current survey design for estimating reproductive output by counting HY birds at sea may not be effective given the high CVs and large confidence limits associated with annual estimates, regardless of which metric is used. Additionally, almost nothing is known about post-fledging movements and dispersal of HY murrelets, making any measure of reproductive output involving counting HY birds at sea difficult to interpret (Lorenz and Raphael, 2018). Density surface model results indicated that HY murrelets were detected primarily near Point Año Nuevo and possibly closer to shore than AHY murrelets throughout the study area (figs. 8, 10). Future survey effort targeting HY murrelets could prioritize these areas, which might be accomplished by increasing alongshore effort as described in the previous section, although encounter rates may remain too low and variable to generate meaningful estimates or to measure trend. Density surface model results developed here could also be used to simulate the efficacy of new survey designs specifically targeting HY murrelets (Rachowicz and others, 2006).

Summary

We’ve documented that the Zone 6 at-sea murrelet abundance has remained stable for the past 23 years and evaluated how various modifications to current survey design may benefit this monitoring program in the future (summarized in table 7). Despite this apparent stability, the effects of the 2020 CZU wildfire in the Santa Cruz Mountains to nesting murrelets may take time to manifest change in local at-sea abundance, assuming significant loss of nesting habitat results in lower reproductive output or redistribution of birds to outside of the study area, and assuming there is no net immigration of murrelets from outside the study area. Long-term annual monitoring at sea will be critical to determine regional effects of this mega-disturbance event to the local murrelet population. Regionally, disentangling intra- and inter-zone changes or redistributions is challenging because at-sea abundance surveys no longer occur annually in Zones 1–5 (McIver and others, 2021), and the entirety of Zone 6 is not surveyed even though failed-breeding and non-breeding murrelets are known to disperse to waters south of our survey area (Peery and others, 2008). Consistent annual at-sea monitoring across all six Conservation Zones, in conjunction with a synthesized analytical framework and perhaps augmented with tracking of murrelets (for example, Motus) to study inter-Zone movements, could be beneficial for management and conservation of murrelets in Washington, Oregon, and California waters.

Table 7. Potential survey and analytical design changes outlined in the “Discussion” and “Summary” Sections.

[Note that survey design changes assume funding and costs are held constant for simplicity. **Abbreviation**: —, none]

Options	After-hatch-year abundance and trend		Hatch-year abundance and trend	
	Pros	Cons	Pros	Cons
Survey design				
1. Remove offshore effort, reallocate effort to nearshore	Reduced variance due to greater sampling of heterogeneous alongshore murrelet distribution will increase power to detect trends.	—	Potentially greater encounter rates that could increase precision of density and count estimates.	—
2. Reduce study temporal window; number of surveys held constant	Logistically easier for field crew; potentially reduced variance because surveys closer in time; more comparable to Zones 1–5 timing if June.	Past year sample sizes would be reduced for temporally consistent comparisons.	Potentially greater encounter rates if temporal window is July, August, or both.	Potentially lesser encounter rates if temporal window is June.
3. Reduce annual survey sample size in conjunction with (2)	Logistically easier for field crew.	Inability to accommodate future change/increase in variance associated with temporal patterns in abundance.	—	Potentially lesser encounter rates and increased variance due to smaller sample size.
4. Expand alongshore study area to all of Zone 6 in conjunction with (3)	More comparable to Zone 1–5 methods; potential to detect annual or long-term redistributions in the future.	Logistically novel and more challenging; no historical comparison possible with additional areas and nearshore-offshore density gradients unknown.	Potential to detect HY murrelets that may have dispersed outside current study area.	—
Analytical design				
1. Global detection function model	Comprehensive and consistent; improved detection function model with more observations; accommodates annual variability in survey detection process (for example, platform, crew, conditions).	—	Comprehensive and consistent; improved detection function model with more observations; accommodates annual variability in survey detection process (for example, platform, crew, conditions).	—
2. DSM/GAM model-based approach	Reduced variance in annual abundance estimates; relaxation of random uniform sampling assumptions; maps for spatial management applications and interannual spatial changes in density.	More computationally intensive and complex.	Maps for spatial management applications.	More computationally intensive and complex; annual detections too few to produce annual maps or abundance estimates.

References Cited

Becker, B.H., and Beissinger, S.R., 2003, Scale-dependent habitat selection by a nearshore seabird, the marbled murrelet, in a highly dynamic upwelling system: Marine Ecology Progress Series, v. 256, p. 243–255. [Available at https://doi.org/10.3354/meps256243.]

Becker, B.H., Beissinger, S.R., and Carter, H.R., 1997, At-sea density monitoring of marbled murrelets in central California—Methodological considerations: The Condor, v. 99, no. 3, p. 743–755, accessed January 1, 2021, at https://doi.org/10.2307/1370485.

Bellefleur, D., Lee, P., and Ronconi, R.A., 2009, The impact of recreational boat traffic on marbled murrelets (*Brachyramphus marmoratus*): Journal of Environmental Management, v. 90, no. 1, p. 531–538. [Available at https://doi.org/10.1016/j.jenvman.2007.12.002.]

Bird, J.P., Terauds, A., Fuller, R.A., Pascoe, P.P., Travers, T.D., McInnes, J.C., Alderman, R., and Shaw, J.D., 2022, Generating unbiased estimates of burrowing seabird populations: Ecography, v. 2022, no. 7, 12 p. [Available at https://doi.org/10.1111/ecog.06204.]

Buckland, S.T., Anderson, D.R., Burnham, K.P., Laake, J.L., Borchers, D.L., and Thomas, L., 2001, Introduction to distance sampling—Estimating abundance of biological populations: Oxford, United Kingdom, Oxford University Press, 448 p.

California Department of Fish and Wildlife, 2004, Generalized California coastline—coastn83.shp: California Department of Fish and Wildlife database, accessed October 20, 2017, at https://filelib.wildlife.ca.gov/Public/R7_MR/BASE/Coastn83.zip.

California Department of Fish and Wildlife, 2021, Threatened and endangered species: California Department of Fish and Wildlife website, accessed April 5, 2021, at https://wildlife.ca.gov/Conservation/CESA.

California Department of Forestry and Fire Protection (CAL FIRE), 2021, CZU lightning complex (including Warnella Fire) incident: California Department of Forestry and Fire Protection website, accessed October 26, 2021, at https://www.fire.ca.gov/incidents/2020/8/16/czu-lightning-complex-including-warnella-fire.

eBird, 2021, eBird—An online database of bird distribution and abundance: Ithaca, N.Y., eBird, Cornell Lab of Ornithology, accessed January 19, 2023, at http://www.ebird.org.

Felis, J.J., Adams, J., Horton, C.A., Kelsey, E.C., and White, L.M., 2022a, Abundance and productivity of Marbled Murrelets (*Brachyramphus marmoratus*) off central California during the 2020 and 2021 breeding seasons: U.S. Geological Survey Data Report 1157, 12 p., accessed January 1, 2023, at https://doi.org/10.3133/dr1157.

Felis, J.J., Adams, J., Peery, M.Z., Henry, R.W., Henkel, L.A., Becker, B.H., and Halbert, P., 2022b, Annual marbled murrelet abundance and productivity surveys off central California (Zone 6), 1999–2021 (ver. 4.0, May 2022): U.S. Geological Survey data release, accessed April 8, 2022, at https://doi.org/10.5066/F75B01RW.

Halbert, P., and Singer, S.W., 2017, Marbled Murrelet landscape management plan for Zone 6: Felton, Calif., California Department of Parks and Recreation, 223 p., accessed November 14, 2022, at https://www.parks.ca.gov/?page_id=29911.

Hall, L.A., Palsbøll, P.J., Beissinger, S.R., Harvey, J.T., Bérubé, M., Raphael, M.G., Nelson, S.K., Golightly, R.T., McFarlane-Tranquilla, L., Newman, S.H., and Peery, M.Z., 2009, Characterizing dispersal patterns in a threatened seabird with limited genetic structure: Molecular Ecology, v. 18, no. 24, p. 5074–5085. [Available at https://doi.org/10.1111/j.1365-294X.2009.04416.x.]

Henkel, L., 2004, At-sea distribution of Marbled Murrelets in San Luis Obispo County, California: Oiled Wildlife Care Network, Project 2268–01, 13 p., accessed January 1, 2022, at https://www.researchgate.net/profile/Laird-Henkel/publication/263844940_At-Sea_Distribution_of_Marbled_Murrelets_in_San_Luis_Obispo_County_California/links/0a85e53c00ab4a9815000000/at-Sea-Distribution-of-Marbled-Murrelets-in-San-Luis-Obispo-County-California.pdf.

Henry, R.W., 2017, Murrelet at sea abundance, productivity, and prey resources in Zone 6, chap. 7 *of* Halbert, P., and Singer, S.W., eds., Marbled murrelet landscape management plan for zone 6: Felton, Calif., California Department of Parks and Recreation, p. 145–160. [Available at http://www.parks.ca.gov/pages/29882/files/Z6-Plan_FINAL_MASTER_V14_07-17.pdf.]

Henry, R.W., and Tyler, W.B., 2017, Abundance and productivity of marbled murrelets off central California during the 2013–2016 breeding seasons: Felton, Calif., The Luckenbach and Command Oil Spill Trustees, 12 p.

Lorenz, T.J., and Raphael, M.G., 2018, Declining Marbled Murrelet density, but not productivity, in the San Juan Islands, Washington, USA: The Condor, v. 120, no. 1, p. 201–222. [Available at https://doi.org/10.1650/CONDOR-17-122.1.]

Marques, T.A., Thomas, L., Fancy, S.G., and Buckland, S.T., 2007, Improving estimates of bird density using multiple-covariate distance sampling: The Auk, v. 124, no. 4, p. 1229–1243. [Available at https://doi.org/10.1093/auk/124.4.1229.]

McIver, W.R., Baldwin, J., Lance, M.M., Pearson, S.F., Strong, C., Raphael, M.G., Duarte, A., and Fitzgerald, K., 2022, Marbled Murrelet effectiveness monitoring, Northwest Forest Plan—At-sea Monitoring—2021 summary report: Northwest Forest Plan Interagency Regional Monitoring Program, 25 p.

McIver, W.R., Pearson, S.F., Strong, C., Lance, M.M., Baldwin, J., Lynch, D., Raphael, M.G., Young, R.D., and Johnson, N., 2021, Status and trend of Marbled Murrelet populations in the Northwest Forest Plan area, 2000 to 2018—U.S. Forest Service General Technical Report PNW-STR-996: Portland, Oreg., Pacific Northwest Research Station, U.S. Department of Agriculture, U.S. Forest Service, 37 p.

Miller, D.L., Burt, M.L., Rexstad, E.A., and Thomas, L., 2013, Spatial models for distance sampling data—Recent developments and future directions: Methods in Ecology and Evolution, v. 4, no. 11, p. 1001–1010. [Available at https://doi.org/10.1111/2041-210X.12105.]

Miller, D.L., Rexstad, E., Thomas, L., Marshall, L., and Laake, J.L., 2019, Distance sampling in R: Journal of Statistical Software, v. 89, no. 1, p. 1–28. [Available at https://doi.org/10.18637/jss.v089.i01.]

Nelson, S.K., 2020, Marbled Murrelet (*Brachyramphus marmoratus*), (ver. 1.0), *in* Poole, A.F., and Gill, F.B., eds., Birds of the world: Ithaca, N.Y., Cornell Lab of Ornithology, accessed January 1, 2023, at https://doi.org/10.2173/bow.marmur.01.

Pedersen, E.J., Miller, D.L., Simpson, G.L., and Ross, N., 2019, Hierarchical generalized additive models in ecology—An introduction with mgcv: PeerJ, v. 7, 42 p. [Available at https://doi.org/10.7717/peerj.6876.]

Peery, M.Z., Becker, B.H., and Beissinger, S.R., 2006, Combining demographic and count-based approaches to identify source-sink dynamics of a threatened seabird: Ecological Applications, v. 16, no. 4, p. 1516–1528, accessed November 1, 2021, at https://doi.org/10.1890/1051-0761(2006)016[1516:CDACAT]2.0.CO;2.

Peery, M.Z., Becker, B.H., and Beissinger, S.R., 2007, Age ratios as estimators of productivity—Testing assumptions on a threatened seabird, the Marbled Murrelet (*Brachyramphus marmoratus*): The Auk, v. 124, no. 1, p. 224–240, accessed November 1, 2021, at https://doi.org/10.1093/auk/124.1.224.

Peery, M.Z., Henkel, L.A., Newman, S.H., Becker, B.H., Harvey, J.T., Thompson, C.W., and Beissinger, S.R., 2008, Effects of rapid flight-feather molt on postbreeding dispersal in a pursuit-diving seabird: The Auk, v. 125, no. 1, p. 113–123. [Available at https://doi.org/10.1525/auk.2008.125.1.113.]

Peery, M.Z., Newman, S.H., Storlazzi, C.D., and Beissinger, S.R., 2009, Meeting reproductive demands in a dynamic upwelling system—Foraging strategies of a pursuit-diving seabird, the Marbled Murrelet: The Condor, v. 111, no. 1, p. 120–134, accessed January 1, 2021, at https://doi.org/10.1525/cond.2009.080094.

Rachowicz, L.J., Hubbard, A.E., and Beissinger, S.R., 2006, Evaluating at-sea sampling designs for Marbled Murrelets using a spatially explicit model: Ecological Modelling, v. 196, nos. 3–4, p. 329–344. [Available at https://doi.org/10.1016/j.ecolmodel.2006.02.011.]

Ralph, C.J., and Miller, S.L., 1995, Offshore population estimates of Marbled Murrelets in California, chap. 33 *of* Ralph, C.J., Hunt, G.L., Jr., Raphael, M.G., and Piatt, J.F., eds., Ecology and conservation of the Marbled Murrelet—U.S. Forest Service General Technical Report PSW-GTR-152: Albany, Calif., Pacific Southwest Research Station, U.S. Department of Agriculture, U.S. Forest Service, p. 353–360. [Available at https://doi.org/10.2737/PSW-GTR-152.]

R Core Team, 2016, R—A language and environment for statistical computing: Vienna, Austria, R Foundation for Statistical Computing, accessed November 1, 2021, at https://www.R-project.org/.

Schmidt, J.H., and Deacy, W.W., 2021, Using spatial distance sampling models to optimize survey effort and address violations of the design assumption: Ecological Solutions and Evidence, v. 2, no. 3, 10 p. [Available at https://doi.org/10.1002/2688-8319.12091.]

Strong, C.S., Keitt, B.S., McIver, W.R., Palmer, C.J., and Gaffney, I., 1995, Distribution and population estimates of Marbled Murrelets at sea in Oregon during the summers of 1992 and 1993, chap. 32 *of* Ralph, C.J., Hunt, G.L., Jr., Raphael, M.G., and Piatt, J.F., eds., Ecology and conservation of the Marbled Murrelet—U.S. Forest Service General Technical Report PSW-GTR-152: Albany, Calif., Pacific Southwest Research Station, U.S. Department of Agriculture, U.S. Forest Service, p. 339–352. [Available at https://doi.org/10.2737/PSW-GTR-152.]

U.S. Fish and Wildlife Service, 1997, Recovery plan for the threatened Marbled Murrelet (*Brachyramphus marmoratus*) in Washington, Oregon, and California: Portland, Oreg., U.S. Fish and Wildlife Service, 202 p.

U.S. Fish and Wildlife Service, 2021, Environmental conservation online system—Marbled Murrelet (*Brachyramphus marmoratus*): U.S. Fish and Wildlife Service website, accessed April 1, 2022, at https://ecos.fws.gov/ecp/species/4467.

Vásquez-Carrillo, C., Henry, R.W., Henkel, L., and Peery, M.Z., 2013, Integrating population and genetic monitoring to understand changes in the abundance of a threatened seabird: Biological Conservation, v. 167, p. 173–178. [Available at https://doi.org/10.1016/j.biocon.2013.08.008.]

Appendix 1.

Survey-Specific Information and Additional Summaries

Table 1.1. Total linear effort, nearshore stratum linear effort, offshore stratum linear effort, total count of after-hatch-year (AHY) murrelets (and number of detections of unique groups), and total count of hatch-year (HY) murrelets for all standardized zig-zag Marbled Murrelet (*Brachyramphus marmoratus*) surveys done in central California Conservation Zone 6 (Half Moon Bay to Santa Cruz, CA) from 1999 to 2021, during the June 1–August 24 survey season.

[Note that all HY murrelets occurred singly or grouped with AHY murrelets. **Abbreviations**: mm/dd/yyyy, month/day/year; km, kilometer]

Date (mm/dd/yyyy)	Total effort (km)	Nearshore effort (km)	Offshore effort (km)	Total AHY murrelets (detections)	Total HY murrelets
1999					
06/30/1999[1]	112.1	87.6	24.5	26 (17)	1
07/19/1999[1,2]	104.4	85.0	19.4	58 (33)	2
07/26/1999[1,2]	98.9	81.3	17.6	59 (31)	3
07/29/1999[2]	96.4	77.4	19.0	38 (22)	0
08/16/1999[2]	93.3	77.8	15.5	42 (29)	0
2000					
06/06/2000	95.3	74.9	20.4	22 (13)	0
06/26/2000	97.5	82.4	15.1	29 (17)	0
06/28/2000	94.1	77.8	16.3	64 (36)	0
07/08/2000	97.6	84.7	12.9	60 (33)	3
07/14/2000[2]	93.7	80.7	13.0	42 (25)	0
07/30/2000[2]	97.9	84.9	13.0	37 (23)	1
08/08/2000[2]	93.8	78.4	15.4	51 (31)	1
08/10/2000[2]	97.1	87.4	9.7	13 (8)	0
2001					
06/21/2001	98.8	68.8	30.0	41 (27)	0
06/26/2001	99.9	69.9	30.0	78 (38)	1
06/28/2001	98.9	79.9	19.0	35 (21)	0
07/03/2001	97.4	75.7	21.7	54 (33)	3
07/05/2001	96.6	77.4	19.2	49 (29)	2
07/07/2001	103.7	82.0	21.7	52 (27)	0
07/09/2001	101.9	80.4	21.5	93 (55)	1
07/11/2001[2]	103.6	78.8	24.8	35 (13)	0
07/13/2001[2]	101.2	81.9	19.3	68 (38)	2
07/17/2001[2]	102.6	82.3	20.3	48 (29)	4
07/22/2001[2]	102.3	84.7	17.6	22 (15)	1
07/23/2001[2]	104.6	87.4	17.2	53 (31)	1
08/10/2001[2]	102.7	85.6	17.1	58 (29)	1
08/11/2001[1,2]	104.0	83.6	20.4	68 (31)	2
08/19/2001[2]	102.3	88.8	13.5	42 (26)	2

Table 1.1. Total linear effort, nearshore stratum linear effort, offshore stratum linear effort, total count of after-hatch-year (AHY) murrelets (and number of detections of unique groups), and total count of hatch-year (HY) murrelets for all standardized zig-zag Marbled Murrelet (*Brachyramphus marmoratus*) surveys done in central California Conservation Zone 6 (Half Moon Bay to Santa Cruz, CA) from 1999 to 2021, during the June 1–August 24 survey season.—Continued

[Note that all HY murrelets occurred singly or grouped with AHY murrelets. **Abbreviations**: mm/dd/yyyy, month/day/year; km, kilometer]

Date (mm/dd/yyyy)	Total effort (km)	Nearshore effort (km)	Offshore effort (km)	Total AHY murrelets (detections)	Total HY murrelets
2002					
06/11/2002[1]	100.2	80.3	19.9	35 (22)	0
06/22/2002	104.0	82.0	22.0	30 (17)	0
06/25/2002	102.6	80.1	22.5	37 (18)	0
07/01/2002[1]	96.4	75.5	20.9	31 (20)	0
07/12/2002[2]	100.6	80.5	20.1	65 (36)	2
07/19/2002[2]	102.0	81.5	20.5	38 (23)	0
07/22/2002[2]	103.2	81.5	21.7	72 (42)	3
07/23/2002[2]	102.6	81.2	21.4	72 (44)	2
07/24/2002[2]	102.5	79.9	22.6	42 (24)	0
07/29/2002[2]	99.2	75.5	23.7	30 (19)	1
07/30/2002[2]	97.3	78.6	18.7	50 (29)	1
08/07/2002[1,2]	96.2	76.6	19.6	34 (21)	1
08/09/2002[2]	98.0	78.6	19.4	56 (29)	2
08/12/2002[2]	96.0	74.4	21.6	57 (34)	1
08/15/2002[2]	102.3	88.6	13.7	78 (42)	2
2003					
06/10/2003	96.6	75.1	21.5	44 (30)	0
06/13/2003	98.0	78.6	19.4	44 (26)	0
06/25/2003	94.9	72.7	22.2	42 (23)	0
06/26/2003	93.3	68.9	24.4	40 (25)	0
07/17/2003[2]	97.2	69.7	27.5	22 (12)	0
07/20/2003[2]	102.6	80.1	22.5	47 (31)	2
07/21/2003[2]	93.1	76.8	16.3	47 (28)	1
07/23/2003[2]	97.2	78.3	18.9	67 (36)	1
07/28/2003[2]	99.1	77.5	21.6	53 (32)	0
07/29/2003[2]	101.3	79.2	22.1	83 (48)	2
07/30/2003[2]	92.9	74.5	18.4	54 (23)	2
08/04/2003[2]	97.6	78.3	19.3	60 (32)	2
2007					
06/20/2007	102.3	88.6	13.7	21 (15)	0
07/10/2007[2]	102.6	81.3	21.3	34 (18)	2
07/12/2007[2]	93.3	68.9	24.4	42 (25)	0
07/19/2007[2]	96.1	77.2	18.9	44 (27)	0
2008					
07/16/2008[2]	101.1	78.7	22.4	18 (13)	0
07/22/2008[2]	90.9	70.3	20.6	26 (13)	0
08/06/2008[2]	99.1	77.5	21.6	4 (4)	0
08/12/2008[2]	96.1	77.2	18.9	12 (8)	0

Table 1.1. Total linear effort, nearshore stratum linear effort, offshore stratum linear effort, total count of after-hatch-year (AHY) murrelets (and number of detections of unique groups), and total count of hatch-year (HY) murrelets for all standardized zig-zag Marbled Murrelet (*Brachyramphus marmoratus*) surveys done in central California Conservation Zone 6 (Half Moon Bay to Santa Cruz, CA) from 1999 to 2021, during the June 1–August 24 survey season.—Continued

[Note that all HY murrelets occurred singly or grouped with AHY murrelets. **Abbreviations**: mm/dd/yyyy, month/day/year; km, kilometer]

Date (mm/dd/yyyy)	Total effort (km)	Nearshore effort (km)	Offshore effort (km)	Total AHY murrelets (detections)	Total HY murrelets
2009					
06/02/2009	102.3	88.6	13.7	58 (37)	0
06/08/2009	97.4	73.3	24.1	28 (20)	0
06/26/2009	95.8	76.5	19.3	53 (32)	0
07/03/2009	95.8	76.5	19.3	47 (28)	1
07/15/2009[2]	96.6	75.1	21.5	72 (43)	0
07/16/2009[2]	97.8	70.6	27.2	73 (41)	1
08/06/2009[2]	104.0	82.0	22.0	36 (19)	0
08/11/2009[2]	103.0	84.3	18.7	34 (20)	2
2010					
06/04/2010	101.7	80.3	21.4	70 (41)	0
06/14/2010	102.0	75.8	26.2	27 (17)	0
06/28/2010	101.2	79.6	21.6	34 (18)	1
07/08/2010	99.1	77.5	21.6	59 (36)	2
07/22/2010[2]	95.8	76.5	19.3	51 (32)	2
07/23/2010[2]	95.8	74.5	21.3	54 (33)	3
07/29/2010[2]	100.6	80.5	20.1	46 (26)	0
2011					
06/02/2011	96.6	75.1	21.5	19 (14)	0
06/21/2011	99.2	75.5	23.7	31 (18)	0
07/06/2011	101.2	80.2	21.0	32 (19)	0
07/28/2011[2]	102.2	80.2	22.0	30 (19)	1
08/11/2011[2]	97.3	78.5	18.8	28 (18)	1
08/22/2011[2]	101.8	81.4	20.4	40 (26)	3
2012					
06/19/2012	101.7	80.3	21.4	48 (30)	0
06/25/2012	101.8	81.4	20.4	48 (31)	1
06/30/2012	102.2	80.2	22.0	48 (27)	0
07/15/2012[2]	95.8	74.5	21.3	43 (23)	1
07/23/2012[2]	101.2	79.6	21.6	31 (18)	0
08/16/2012[2]	97.4	73.3	24.1	22 (11)	0
2013					
06/05/2013	97.3	78.5	18.8	45 (27)	0
06/24/2013	104.0	82.0	22.0	89 (52)	4
07/08/2013	95.8	76.5	19.3	57 (29)	3
07/17/2013[2]	99.1	77.5	21.6	58 (35)	1
07/23/2013[2]	102.2	80.2	22.0	75 (44)	3
08/20/2013[2]	103.8	77.5	26.3	12 (11)	5

Table 1.1. Total linear effort, nearshore stratum linear effort, offshore stratum linear effort, total count of after-hatch-year (AHY) murrelets (and number of detections of unique groups), and total count of hatch-year (HY) murrelets for all standardized zig-zag Marbled Murrelet (*Brachyramphus marmoratus*) surveys done in central California Conservation Zone 6 (Half Moon Bay to Santa Cruz, CA) from 1999 to 2021, during the June 1–August 24 survey season.—Continued

[Note that all HY murrelets occurred singly or grouped with AHY murrelets. **Abbreviations**: mm/dd/yyyy, month/day/year; km, kilometer]

Date (mm/dd/yyyy)	Total effort (km)	Nearshore effort (km)	Offshore effort (km)	Total AHY murrelets (detections)	Total HY murrelets
2014					
06/27/2014	104.0	82.0	22.0	41 (25)	0
07/01/2014	102.2	80.2	22.0	22 (13)	0
07/08/2014	99.1	77.5	21.6	67 (40)	2
07/15/2014[2]	95.8	76.5	19.3	63 (38)	0
07/22/2014[2]	97.3	78.5	18.8	62 (28)	2
07/26/2014[2]	101.8	81.4	20.4	59 (32)	2
08/12/2014[2]	103.8	77.5	26.3	30 (18)	2
08/16/2014[2]	101.2	79.6	21.6	44 (25)	7
08/21/2014[2]	96.6	75.1	21.5	10 (7)	0
2015					
06/01/2015	94.2	74.0	20.2	29 (18)	0
06/08/2015	103.8	77.5	26.3	22 (15)	0
07/07/2015	97.3	78.5	18.8	69 (35)	0
07/16/2015[2]	101.8	81.4	20.4	31 (20)	0
07/21/2015[2]	95.8	76.5	19.3	29 (18)	1
07/29/2015[2]	99.1	77.5	21.6	20 (13)	1
08/04/2015[2]	101.2	79.6	21.6	9 (7)	0
08/05/2015[2]	104.0	82.0	22.0	12 (8)	1
08/11/2015[2]	101.7	80.3	21.4	26 (16)	1
2016					
06/06/2016	97.3	78.5	18.8	94 (47)	0
07/06/2016	104.0	82.0	22.0	46 (26)	0
07/17/2016[2]	96.6	75.1	21.5	62 (34)	1
07/26/2016[2]	103.8	77.5	26.3	33 (18)	0
08/02/2016[2]	95.8	76.5	19.3	34 (21)	4
08/03/2016[2]	101.8	81.4	20.4	34 (19)	5
08/22/2016[2]	101.2	79.6	21.6	22 (13)	1
2017					
06/07/2017	101.2	79.6	21.6	19 (13)	0
06/19/2017	104.0	82.0	22.0	25 (16)	0
06/22/2017	99.1	77.5	21.6	16 (16)	0
07/12/2017[2]	102.2	80.2	22.0	39 (23)	1
07/23/2017[2]	101.2	79.6	21.6	55 (28)	0
07/26/2017[2]	103.8	77.5	26.3	42 (25)	0
08/01/2017[2]	97.3	78.5	18.8	63 (33)	0
08/09/2017[2]	95.8	76.5	19.3	31 (18)	0
08/18/2017[2]	101.8	81.4	20.4	43 (26)	2

Table 1.1. Total linear effort, nearshore stratum linear effort, offshore stratum linear effort, total count of after-hatch-year (AHY) murrelets (and number of detections of unique groups), and total count of hatch-year (HY) murrelets for all standardized zig-zag Marbled Murrelet (*Brachyramphus marmoratus*) surveys done in central California Conservation Zone 6 (Half Moon Bay to Santa Cruz, CA) from 1999 to 2021, during the June 1–August 24 survey season.—Continued

[Note that all HY murrelets occurred singly or grouped with AHY murrelets. **Abbreviations**: mm/dd/yyyy, month/day/year; km, kilometer]

Date (mm/dd/yyyy)	Total effort (km)	Nearshore effort (km)	Offshore effort (km)	Total AHY murrelets (detections)	Total HY murrelets
2018					
06/19/2018	97.3	78.5	18.8	42 (26)	0
06/26/2018	99.1	77.5	21.6	39 (23)	0
07/02/2018	102.2	80.2	22.0	15 (11)	0
08/03/2018[2]	102.5	80.6	21.9	46 (27)	0
08/06/2018[2]	101.7	80.3	21.4	13 (8)	0
08/08/2018[2]	96.6	75.1	21.5	16 (10)	2
08/10/2018[2]	101.2	79.6	21.6	15 (11)	0
08/13/2018[2]	103.8	77.5	26.3	26 (15)	2
08/20/2018[2]	101.8	81.4	20.4	23 (15)	0
2019					
06/12/2019	97.3	78.5	18.8	19 (11)	0
06/14/2019	103.1	81.2	21.9	25 (16)	0
07/18/2019[2]	96.6	75.1	21.5	33 (24)	0
07/22/2019[2]	103.8	77.5	26.3	54 (29)	0
08/09/2019[2]	95.8	76.5	19.3	39 (23)	1
08/10/2019[2]	101.8	81.4	20.4	17 (10)	0
08/15/2019[2]	101.2	79.6	21.6	13 (8)	2
08/19/2019[2]	101.7	80.3	21.4	22 (14)	0
2020					
06/18/2020	102.2	80.2	22.0	17 (11)	0
06/23/2020	102.4	84.7	17.7	9 (7)	0
06/25/2020	103.7	82.0	21.7	38 (24)	0
07/20/2020[2]	96.6	75.0	21.6	51 (30)	0
07/21/2020[2]	103.7	79.0	24.7	30 (20)	0
07/29/2020[2]	103.0	85.9	17.1	37 (22)	0
08/12/2020[2]	99.2	75.5	23.7	16 (9)	0
08/13/2020[2]	101.4	82.4	19.0	53 (34)	2
08/15/2020[2]	101.2	81.8	19.4	49 (25)	1
2021					
06/12/2021	101.7	80.3	21.4	13 (11)	0
06/24/2021	104.0	83.5	20.5	20 (12)	0
07/01/2021	98.8	77.0	21.8	30 (18)	0
07/13/2021[2]	103.7	79.0	24.7	7 (5)	0
07/23/2021[2]	95.8	76.5	19.3	28 (16)	0
07/28/2021[2]	102.4	84.7	17.7	76 (43)	1
07/30/2021[2]	97.3	78.5	18.8	30 (17)	0
08/09/2021[2]	101.0	82.0	19.0	10 (7)	2
08/23/2021[2]	103.7	82.0	21.7	10 (6)	1

[1]Survey completed in two days with start date indicated.

[2]Survey included in HY abundance estimation and reproductive index date window (July 10–August 24).

Table 1.2. Observer view conditions classifications and descriptions for at-sea Marbled Murrelet surveys.

[~, about; m, meter]

View condition	Description
5—Excellent	Glassy, no glare
4—Very good	Wavelets, minor glare, or both
3—Good	Small waves/wavelets, minor glare, or both; still able to reliably detect murrelets within ~75 m of line
2—Fair	Waves, moderate glare, or both; chance of missing murrelets within ~75 m of line
1—Poor	High-wind waves, high glare, or both; murrelets difficult to detect

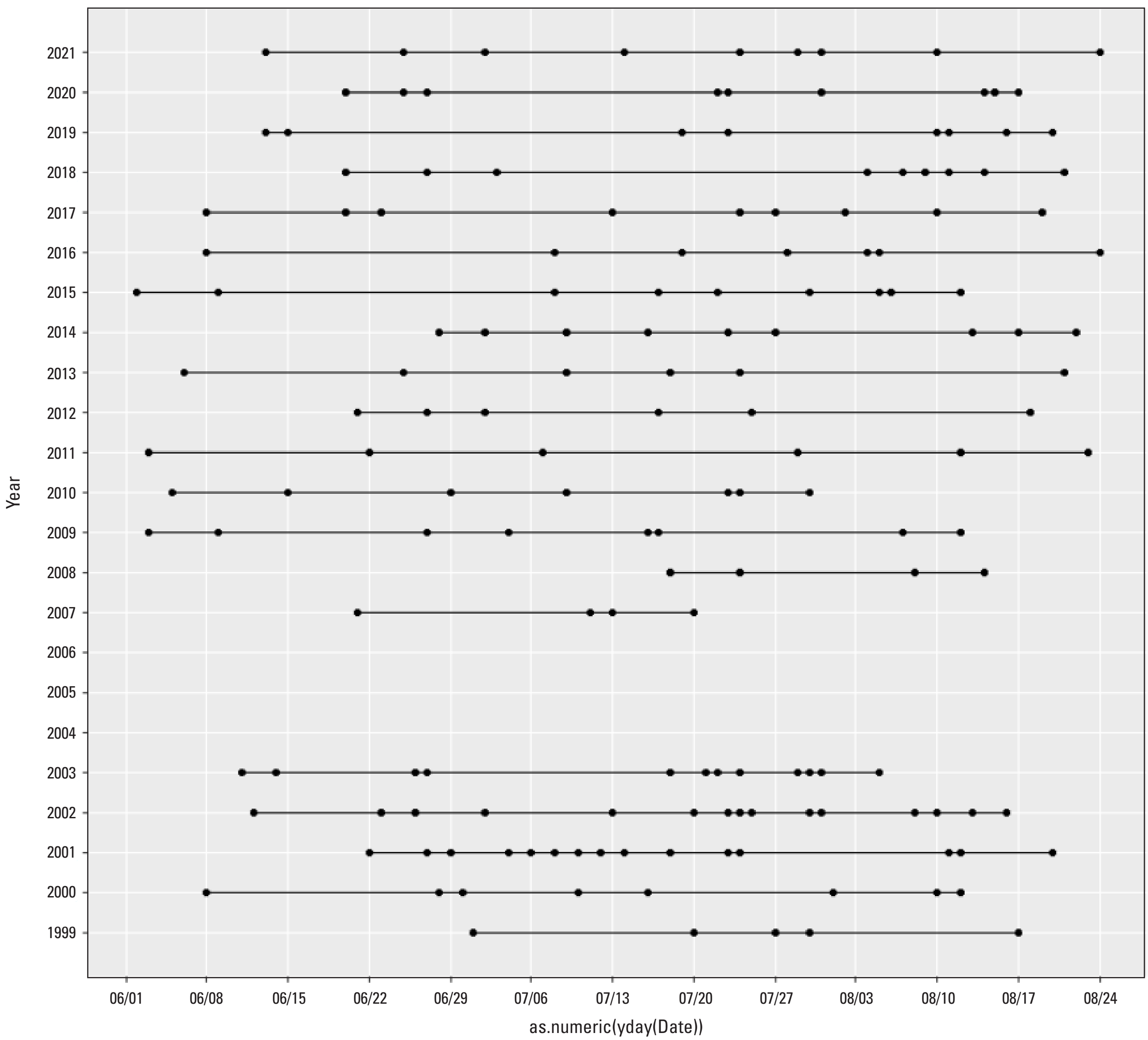

Figure 1.1. Plot showing survey dates for each year.

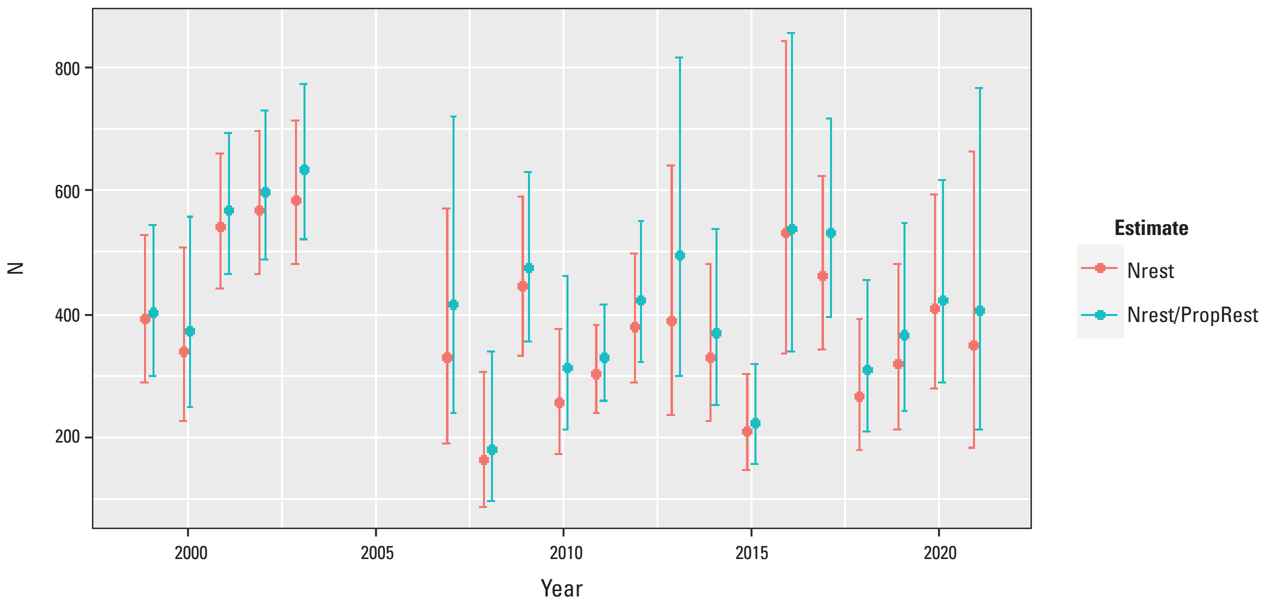

Figure 1.2. Estimated annual abundance (N) of Marbled Murrelets in Zone 6 based on detection functioning modeling using only birds observed resting on the water (Nrest) and with flying birds reincorporated into estimate by dividing the abundance estimate of resting birds by what proportion they were of the total birds indicating both behaviors combined (Nrest/PropRest). Error bars are 95-percent confidence interval.

Density Surface Model Diagnostics and Additional Results

After-Hatch-Year Model Summary and Annual Response Plots

The following text provides a model summary report for the final selected generalized additive model:

```
summary(AHY_dsm_nb_yrGI)
Family: Negative Binomial(0.107)
Link function: log

Formula:
count ~ s(mamu_along, k=25) + s(dstcstmain, k=10) + s(mamu_along,
    by=Year, m=1, k=25) + s(dstcstmain, by=Year, m=1,
    k=10) + s(Year, bs="re," k=NROW(unique(AHY_obs_segs$Year))) +
    offset(off.set)

Parametric coefficients:
            Estimate Std. Error z value Pr(>|z|)
(Intercept) -0.4672      0.1145  -4.079 4.51e-05 ***
---
Signif. codes: 0 '***' 0.001 '**' 0.01 '*' 0.05 '.' 0.1 ' ' 1
```

```
Approximate significance of smooth terms:
                             edf Ref.df  Chi.sq   p-value
s(mamu_along)          1.893e+01 21.286 447.803   < 2e-16 ***
s(dstcstmain)          5.635e+00  6.572 606.342   < 2e-16 ***
s(mamu_along):Year1999 6.573e+00 24.000  15.089 0.028482 *
s(mamu_along):Year2000 1.294e+01 24.000  54.518 1.08e-05 ***
s(mamu_along):Year2001 2.192e-03 24.000   0.001 0.694423
s(mamu_along):Year2002 5.998e+00 24.000  12.943 0.019966 *
s(mamu_along):Year2003 1.311e+01 24.000  48.599 5.87e-05 ***
s(mamu_along):Year2007 7.354e+00 24.000  55.859  < 2e-16 ***
s(mamu_along):Year2008 2.698e+00 24.000   6.339 0.040343 *
s(mamu_along):Year2009 1.108e+01 24.000  39.633 1.17e-05 ***
s(mamu_along):Year2010 1.068e+01 24.000  39.438 5.35e-06 ***
s(mamu_along):Year2011 5.611e+00 24.000  18.170 0.039135 *
s(mamu_along):Year2012 5.958e+00 24.000  31.145 0.008577 **
s(mamu_along):Year2013 2.944e+00 24.000   8.274 0.025545 *
s(mamu_along):Year2014 6.072e+00 24.000  13.359 0.091708 .
s(mamu_along):Year2015 5.971e+00 24.000  70.346 0.000903 ***
s(mamu_along):Year2016 9.620e+00 24.000 242.018 2.71e-05 ***
s(mamu_along):Year2017 5.189e+00 24.000  20.551 0.006047 **
s(mamu_along):Year2018 1.599e+00 24.000   3.059 0.116307
s(mamu_along):Year2019 1.114e+01 24.000  48.431 4.43e-05 ***
s(mamu_along):Year2020 7.548e+00 24.000  78.648 6.30e-05 ***
s(mamu_along):Year2021 1.408e+01 24.000  83.716 2.22e-05 ***
s(dstcstmain):Year1999 9.941e-01  9.000   2.194 0.107345
s(dstcstmain):Year2000 7.222e-04  9.000   0.000 0.698430
s(dstcstmain):Year2001 1.885e+00  9.000  13.208 0.019490 *
s(dstcstmain):Year2002 9.205e-01  9.000   2.683 0.075692 .
s(dstcstmain):Year2003 2.899e-03  9.000   0.002 0.627317
s(dstcstmain):Year2007 1.185e-03  9.000   0.001 0.498820
s(dstcstmain):Year2008 1.950e+00  9.000   9.316 0.007340 **
s(dstcstmain):Year2009 2.763e+00  9.000   8.597 0.059383 .
s(dstcstmain):Year2010 2.920e+00  9.000  18.426 0.000477 ***
s(dstcstmain):Year2011 2.201e-03  9.000   0.001 0.790176
s(dstcstmain):Year2012 1.427e-03  9.000   0.000 0.810097
s(dstcstmain):Year2013 2.219e+00  9.000   8.196 0.014274 *
s(dstcstmain):Year2014 2.322e-03  9.000   0.001 0.849329
s(dstcstmain):Year2015 1.445e-03  9.000   0.000 0.798371
s(dstcstmain):Year2016 8.879e-04  9.000   0.000 0.606053
s(dstcstmain):Year2017 3.125e+00  9.000  13.291 0.001693 **
s(dstcstmain):Year2018 3.384e-02  9.000   0.040 0.283280
s(dstcstmain):Year2019 5.629e+00  9.000  27.621 4.57e-05 ***
s(dstcstmain):Year2020 1.150e-02  9.000   0.010 0.420712
s(dstcstmain):Year2021 2.060e+00  9.000   3.365 0.161206
s(Year)                1.626e+01 19.000 132.623  < 2e-16 ***
---
Signif. codes:  0 '***' 0.001 '**' 0.01 '*' 0.05 '.' 0.1 ' ' 1

R-sq.(adj) = 0.0916  Deviance explained = 39.9%
-REML = 10688 Scale est. = 1 n = 33783
```

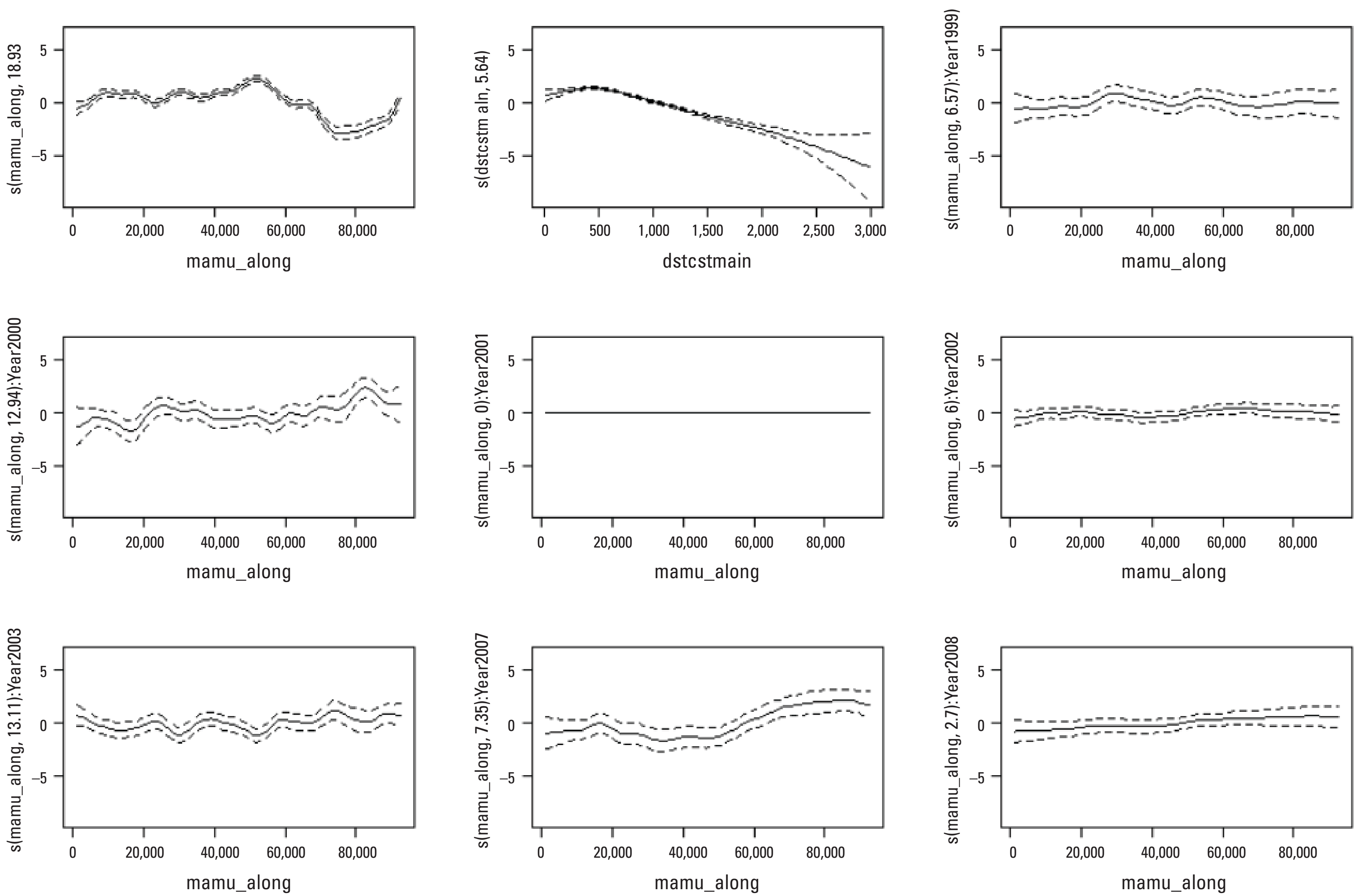

Figure 1.3. Response plots for the final selected generalized additive model ("AHY_dsm_nb_yrGI") predicting after-hatch-year murrelet counts as a function of distance to coast (dstcstmain) and alongshore position (mamu_along). Predictor variables are labeled on the *x*-axes and the predicted responses (murrelet count) on the *y*-axes. *Y*-axes without a year in the label (the first two plots) are the overall response for all years combined, whereas those with year in the *y*-axis label show year-specific responses (specifically, how the year-specific response differs from the overall response).

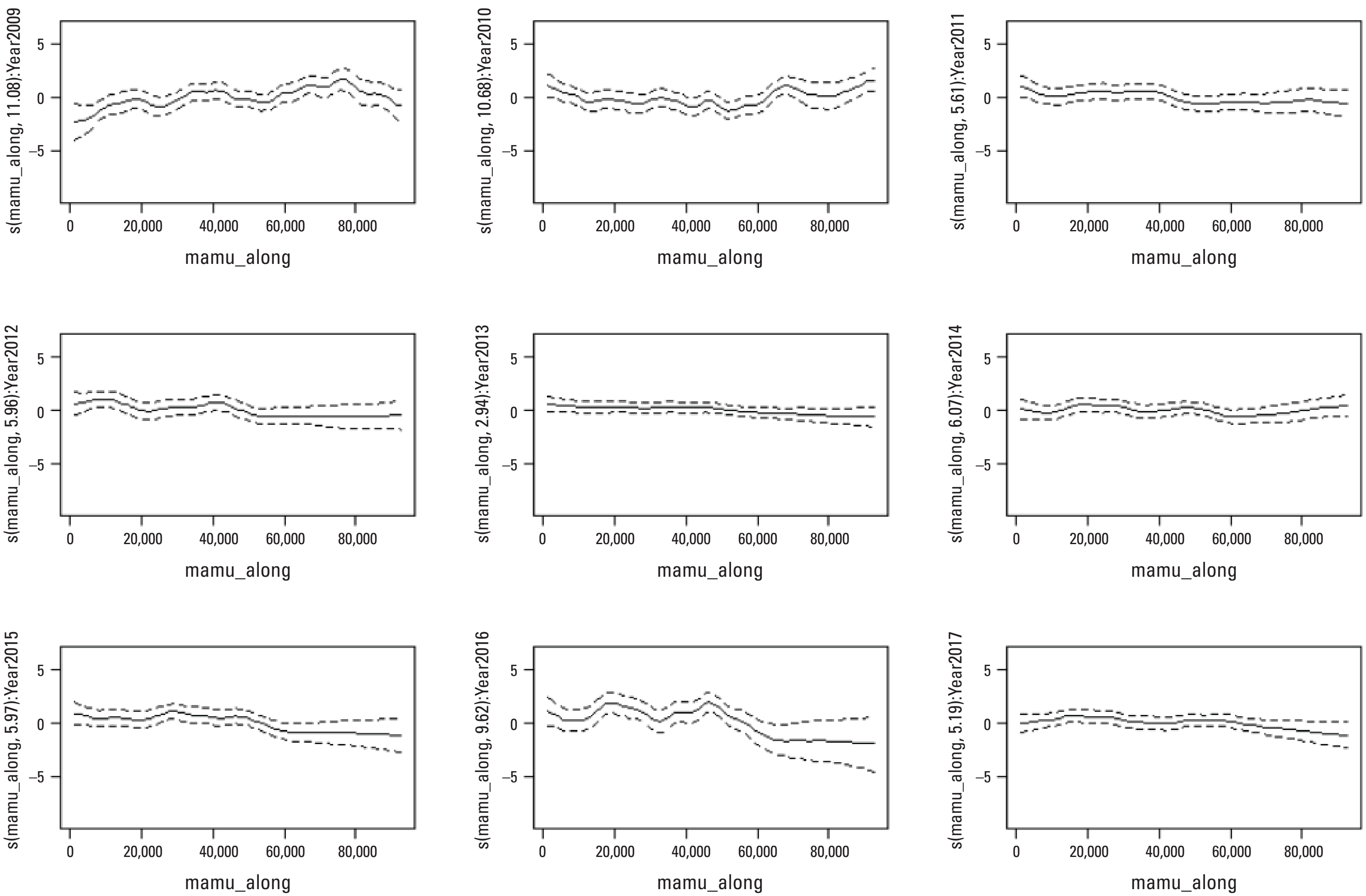

Figure 1.3.—Continued

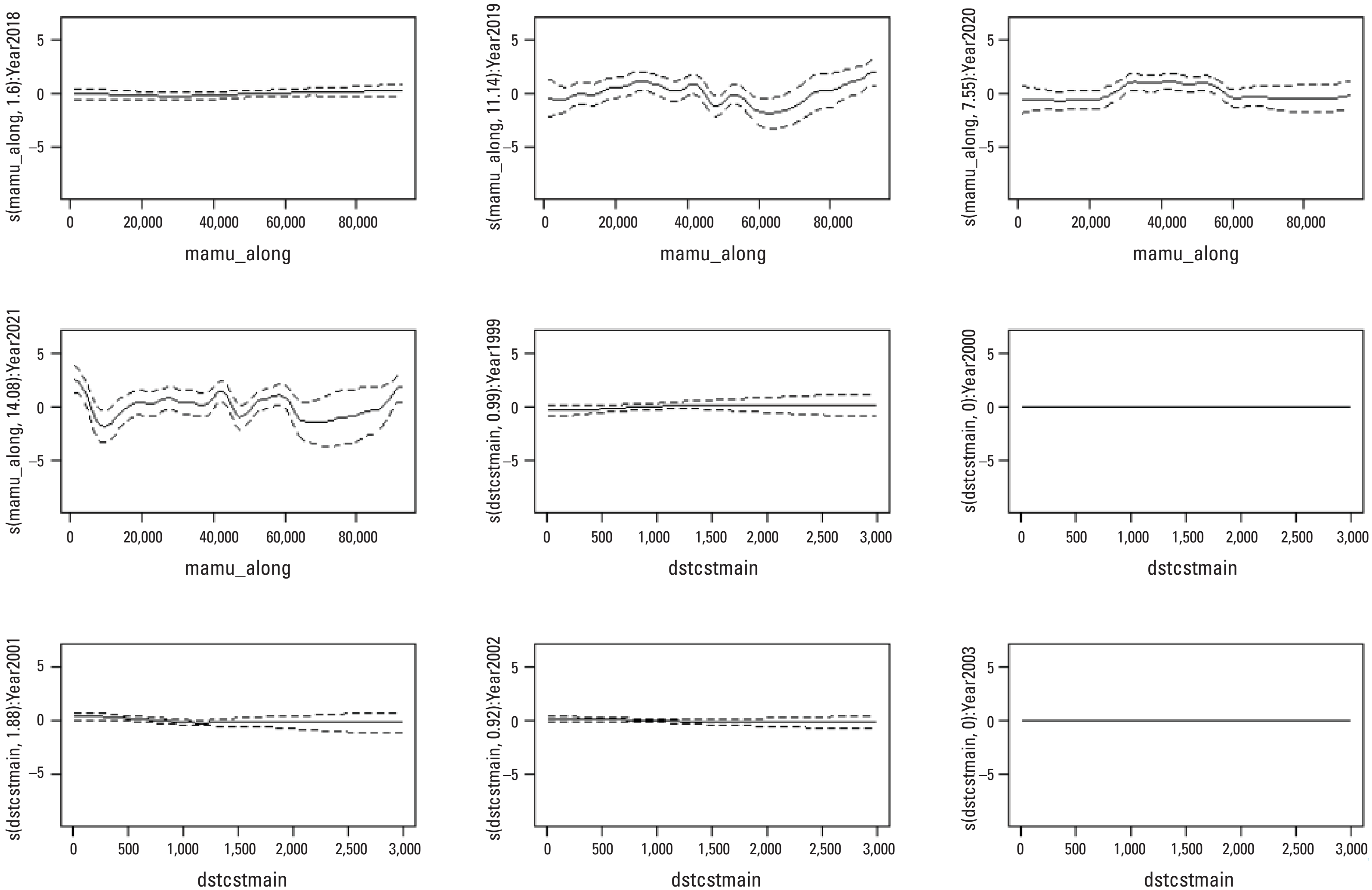

Figure 1.3.—Continued

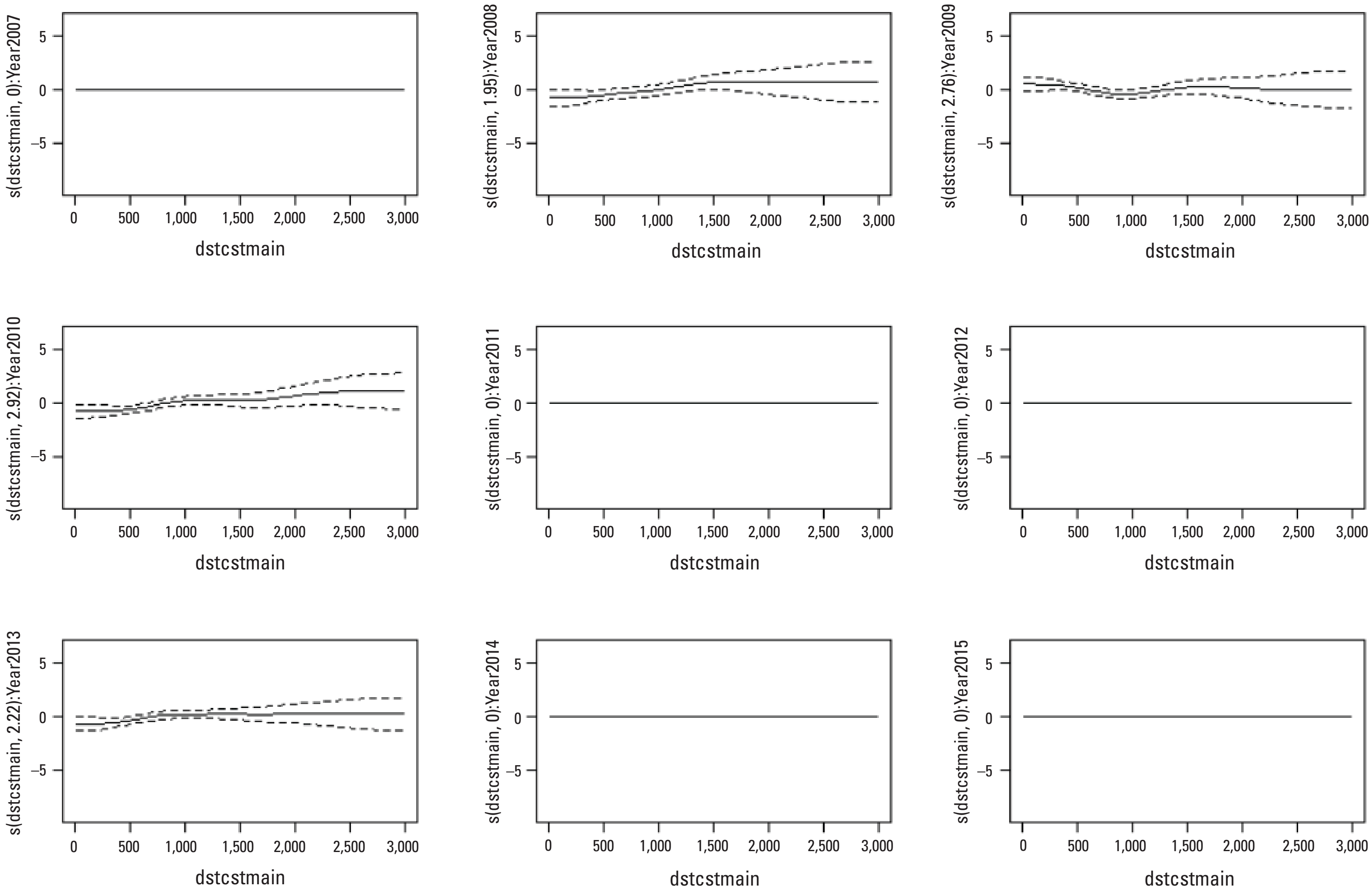

Figure 1.3.—Continued

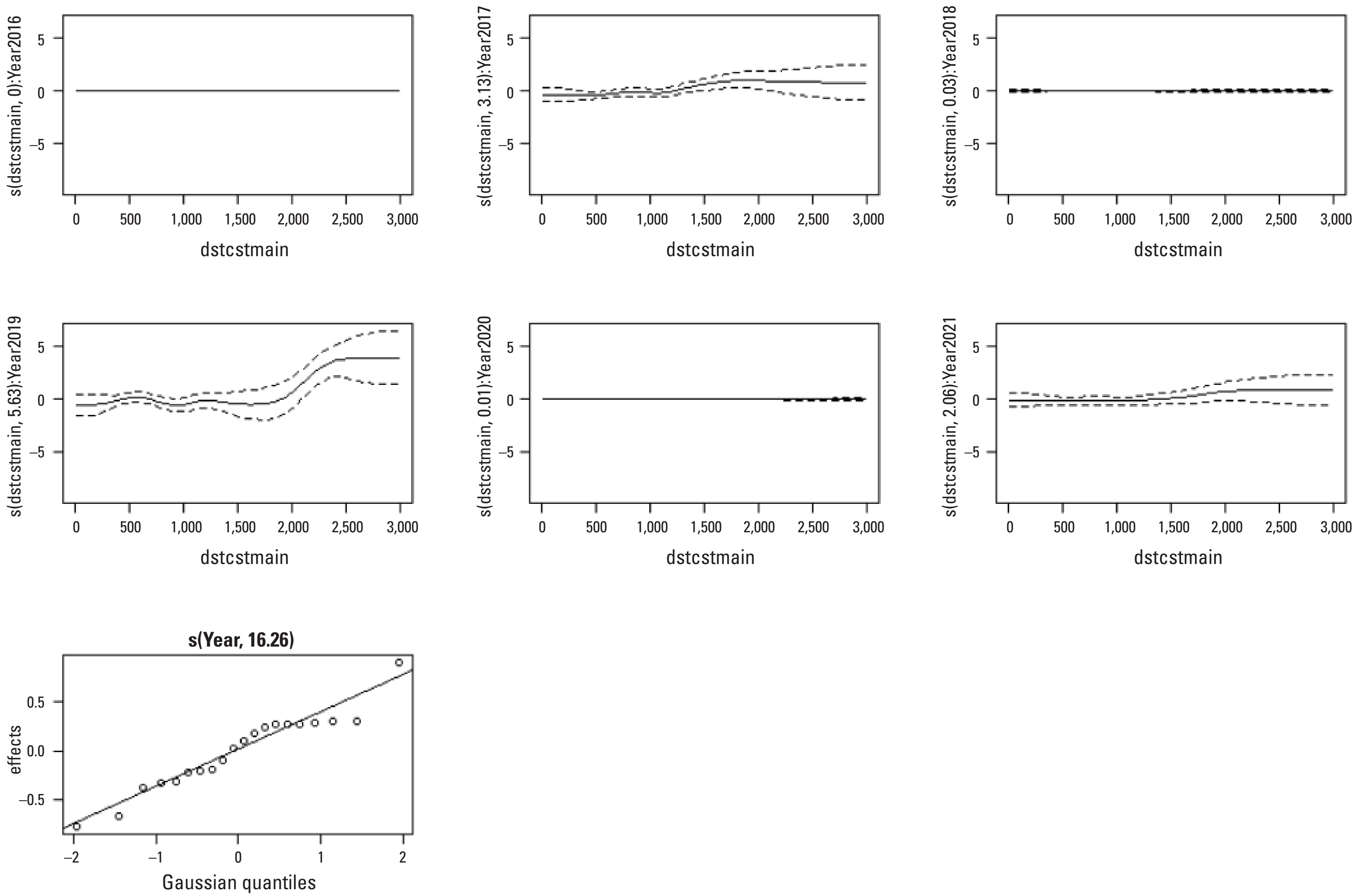

Figure 1.3.—Continued

After-Hatch-Year Model Diagnostic Summaries and Plots

The following text provides a model diagnostic report for the final selected generalized additive model for after-hatch-year murrelets:

```
gam.check(AHY_dsm_nb_yrGI)

Method: REML Optimizer: outer newton
full convergence after 13 iterations.
Gradient range [-0.0008656493,9.215507e-05]
(score 10687.84 & scale 1).
Hessian positive definite, eigenvalue range [0.0001642379,766.9828].
Model rank = 714 / 714

Basis dimension (k) checking results. Low p-value (k-index<1) may
indicate that k is too low, especially if edf is close to k'.

                              k'      edf k-index  p-value
s(mamu_along)          2.40e+01 1.89e+01    0.70   <2e-16 ***
s(dstcstmain)          9.00e+00 5.64e+00    0.71   <2e-16 ***
s(mamu_along):Year1999 2.40e+01 6.57e+00    0.70   <2e-16 ***
s(mamu_along):Year2000 2.40e+01 1.29e+01    0.70   <2e-16 ***
s(mamu_along):Year2001 2.40e+01 2.19e-03    0.70   <2e-16 ***
s(mamu_along):Year2002 2.40e+01 6.00e+00    0.70   <2e-16 ***
s(mamu_along):Year2003 2.40e+01 1.31e+01    0.70   <2e-16 ***
s(mamu_along):Year2007 2.40e+01 7.35e+00    0.70   <2e-16 ***
s(mamu_along):Year2008 2.40e+01 2.70e+00    0.70   <2e-16 ***
s(mamu_along):Year2009 2.40e+01 1.11e+01    0.70   <2e-16 ***
s(mamu_along):Year2010 2.40e+01 1.07e+01    0.70   <2e-16 ***
s(mamu_along):Year2011 2.40e+01 5.61e+00    0.70   <2e-16 ***
s(mamu_along):Year2012 2.40e+01 5.96e+00    0.70   <2e-16 ***
s(mamu_along):Year2013 2.40e+01 2.94e+00    0.70   <2e-16 ***
s(mamu_along):Year2014 2.40e+01 6.07e+00    0.70    0.005 **
s(mamu_along):Year2015 2.40e+01 5.97e+00    0.70   <2e-16 ***
s(mamu_along):Year2016 2.40e+01 9.62e+00    0.70   <2e-16 ***
s(mamu_along):Year2017 2.40e+01 5.19e+00    0.70   <2e-16 ***
s(mamu_along):Year2018 2.40e+01 1.60e+00    0.70   <2e-16 ***
s(mamu_along):Year2019 2.40e+01 1.11e+01    0.70   <2e-16 ***
s(mamu_along):Year2020 2.40e+01 7.55e+00    0.70   <2e-16 ***
s(mamu_along):Year2021 2.40e+01 1.41e+01    0.70   <2e-16 ***
s(dstcstmain):Year1999 9.00e+00 9.94e-01    0.71    0.005 **
s(dstcstmain):Year2000 9.00e+00 7.22e-04    0.71    0.005 **
s(dstcstmain):Year2001 9.00e+00 1.88e+00    0.71   <2e-16 ***
s(dstcstmain):Year2002 9.00e+00 9.20e-01    0.71    0.005 **
s(dstcstmain):Year2003 9.00e+00 2.90e-03    0.71    0.005 **
s(dstcstmain):Year2007 9.00e+00 1.19e-03    0.71    0.015 *
s(dstcstmain):Year2008 9.00e+00 1.95e+00    0.71    0.010 **
s(dstcstmain):Year2009 9.00e+00 2.76e+00    0.71    0.010 **
s(dstcstmain):Year2010 9.00e+00 2.92e+00    0.71    0.005 **
s(dstcstmain):Year2011 9.00e+00 2.20e-03    0.71    0.005 **
s(dstcstmain):Year2012 9.00e+00 1.43e-03    0.71    0.010 **
s(dstcstmain):Year2013 9.00e+00 2.22e+00    0.71   <2e-16 ***
s(dstcstmain):Year2014 9.00e+00 2.32e-03    0.71    0.005 **
s(dstcstmain):Year2015 9.00e+00 1.45e-03    0.71    0.005 **
s(dstcstmain):Year2016 9.00e+00 8.88e-04    0.71    0.005 **
s(dstcstmain):Year2017 9.00e+00 3.13e+00    0.71    0.005 **
s(dstcstmain):Year2018 9.00e+00 3.38e-02    0.71    0.005 **
s(dstcstmain):Year2019 9.00e+00 5.63e+00    0.71    0.010 **
s(dstcstmain):Year2020 9.00e+00 1.15e-02    0.71   <2e-16 ***
s(dstcstmain):Year2021 9.00e+00 2.06e+00    0.71   <2e-16 ***
s(Year)                2.00e+01 1.63e+01      NA       NA
---
Signif. codes: 0 '***' 0.001 '**' 0.01 '*' 0.05 '.' 0.1 ' ' 1
```

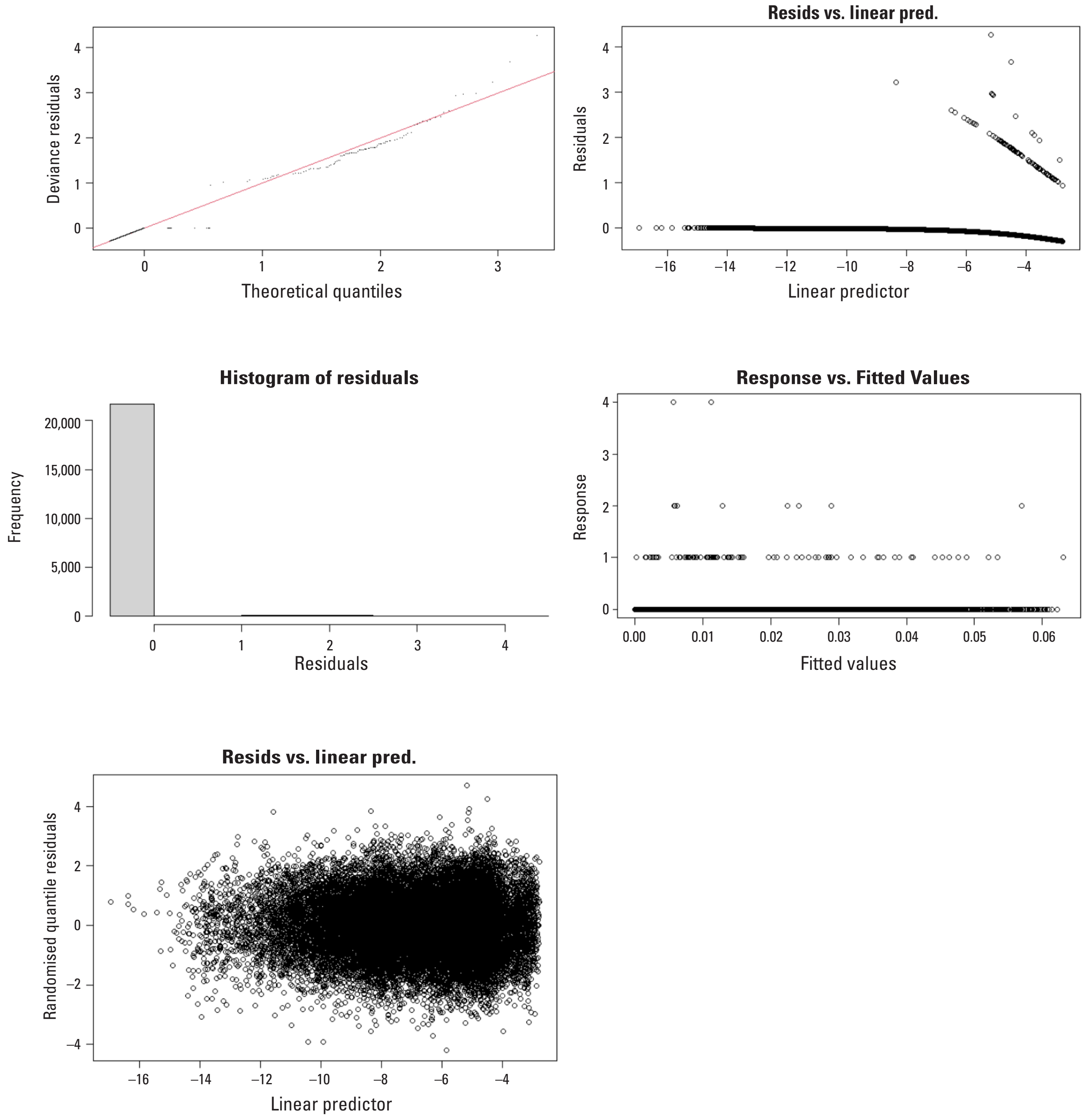

Figure 1.4. Diagnostic plots for the final selected generalized additive model ("AHY_dsm_nb_yrGI") predicting after-hatch-year murrelet counts.

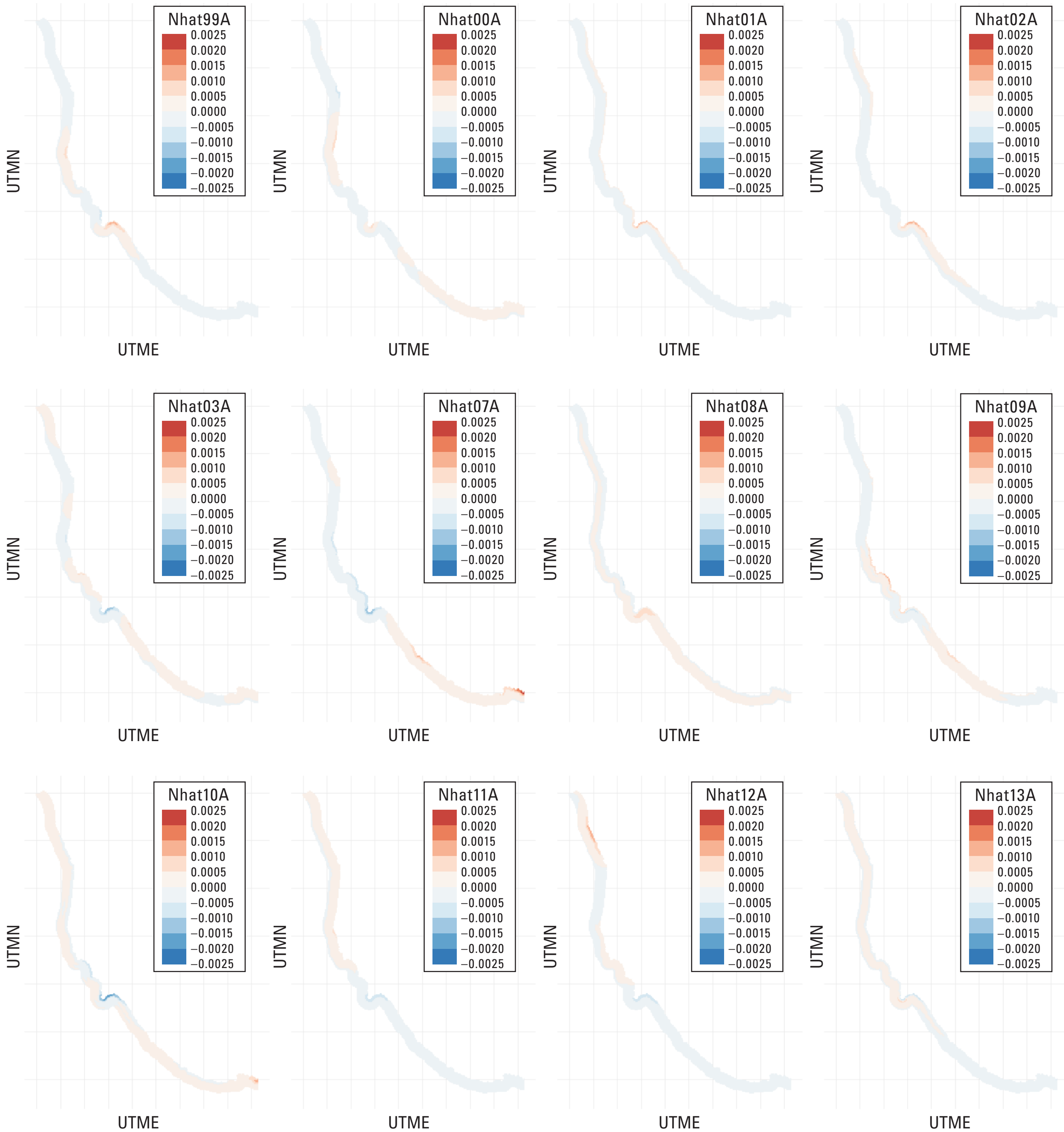

Figure 1.5. Annual anomalies of after-hatch-year (AHY) Marbled Murrelet density surface model (DSM) results (annual DSM prediction minus long-term average DSM prediction) for all study years. Annual and long-term-average DSMs were divided by their respective sums to standardize before calculating anomaly.

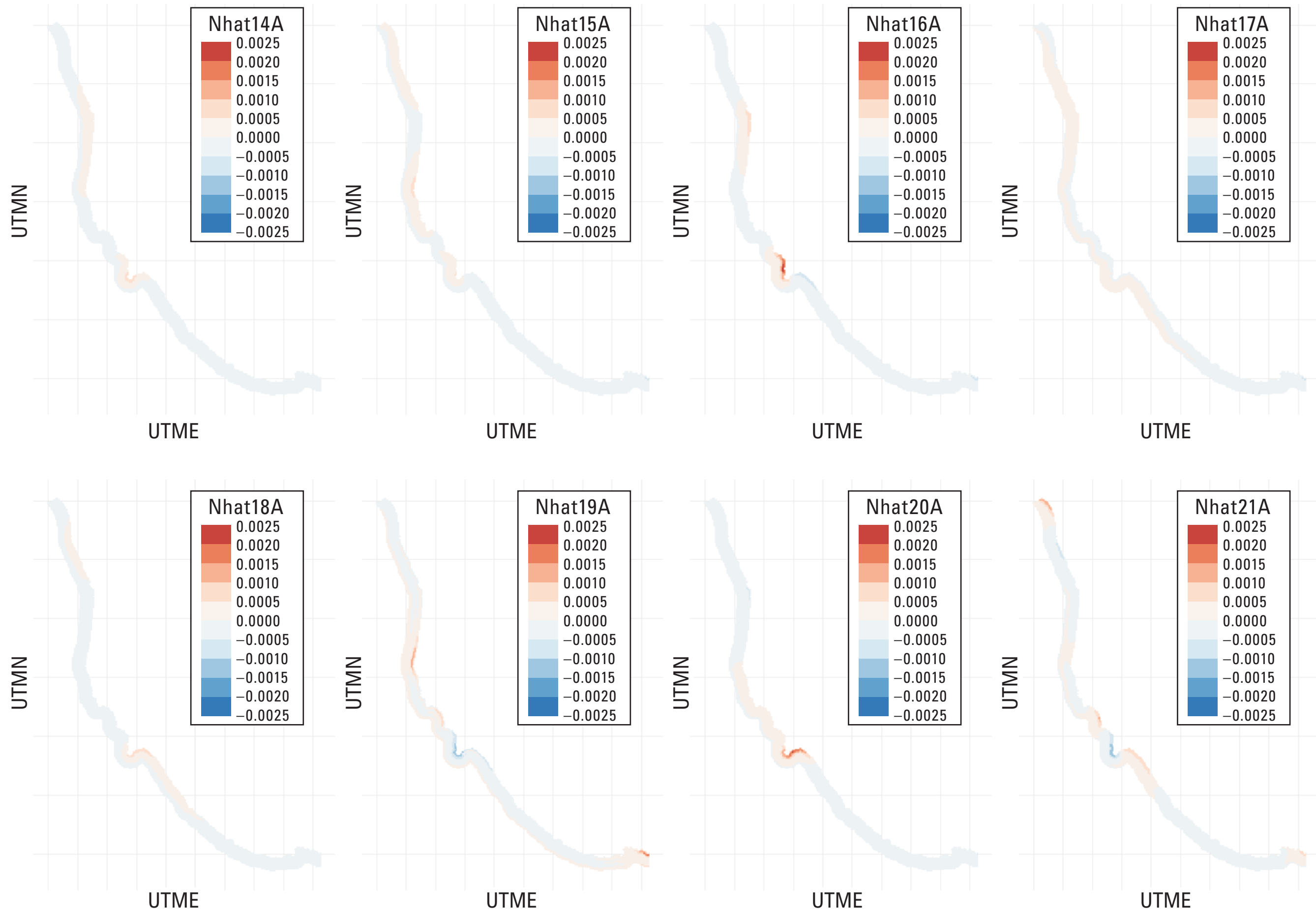

Figure 1.5.—Continued

After-Hatch-Year Annual Distribution Anomaly Maps

We divided each annual Marbled Murrelet spatial density prediction layer by its sum to standardize, and then subtracted the long-term average predicted density for all years (also standardized by dividing by its sum) to generate annual spatial anomaly maps (fig. 1.5). These mapped anomalies indicate distribution differences each year, independent of overall annual density/abundance. Positive and negative values indicate greater and lesser relative annual density compared to the long-term average.

Hatch-Year Model Summary and Diagnostics

The following text provides a model summary report for the final selected generalized additive model for hatch-year murrelets (“HY_dsm_nb”):

```
summary(HY_dsm_nb)

Family: Negative Binomial(0.054)
Link function: log

Formula:
count ~ s(mamu_along, k=25) + s(dstcstmain, k=10) + offset(off.set)

Parametric coefficients:
            Estimate Std. Error z value Pr(>|z|)
(Intercept) -3.8684      0.3425  -11.29   <2e-16 ***
---

Signif. codes: 0 '***' 0.001 '**' 0.01 '*' 0.05 '.' 0.1 ' ' 1

Approximate significance of smooth terms:
                edf Ref.df Chi.sq  p-value
s(mamu_along) 8.402 10.441  71.14  < 2e-16 ***
s(dstcstmain) 2.334  2.965  35.10 6.64e-07 ***
---
Signif. codes: 0 '***' 0.001 '**' 0.01 '*' 0.05 '.' 0.1 ' ' 1

R-sq.(adj) = 0.00874   Deviance explained = 26.9%
-REML = 592.59  Scale est. = 1         n = 21789
```

The following text provides a model diagnostic report for the final selected generalized additive model for hatch-year murrelets (“HY_dsm_nb”):

```
gam.check(HY_dsm_nb)

Method: REML   Optimizer: outer newton
full convergence after 6 iterations.
Gradient range [-8.192291e-09,1.314911e-09]
(score 592.5926 & scale 1).
Hessian positive definite, eigenvalue range [0.379771,10.04704].
Model rank =  34 / 34

Basis dimension (k) checking results. Low p-value (k-index<1) may
indicate that k is too low, especially if edf is close to k'.

                 k'   edf  k-index p-value
s(mamu_along) 24.00  8.40    0.82    0.025 *
s(dstcstmain)  9.00  2.33    0.83    0.055 .
---
Signif. codes: 0 '***' 0.001 '**' 0.01 '*' 0.05 '.' 0.1 ' ' 1
```

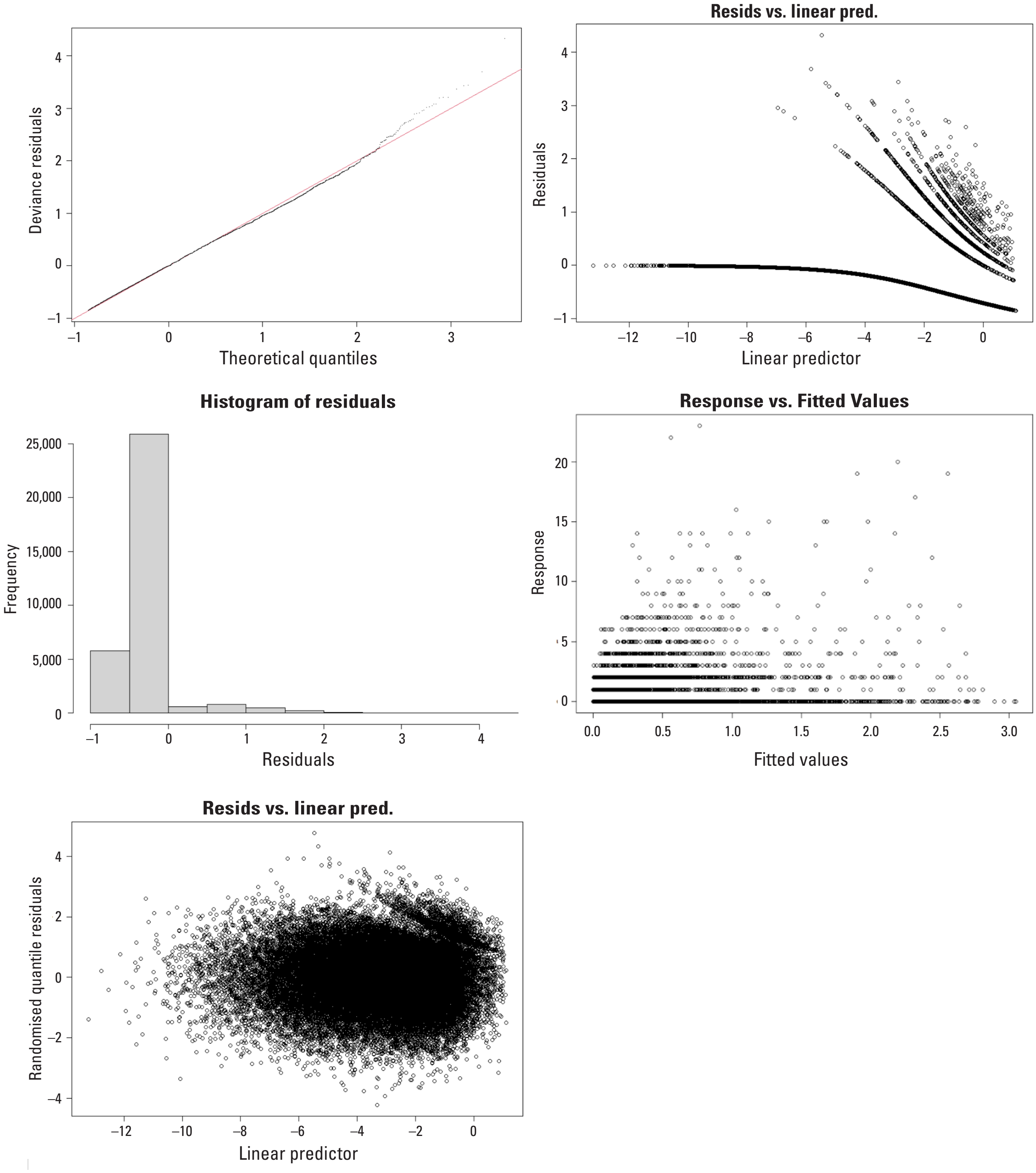

Figure 1.6. Diagnostic plots for the final selected generalized additive model ("HY_dsm_nb") predicting hatch-year murrelet counts.

Hatch-Year to After-Hatch-Year Ratio Calculation Methods

We estimated the juvenile ratio (the ratio of HY to AHY individuals) for Marbled Murrelet surveys completed during the fledging period following methods developed by Peery and others (2007). The previously established fledging period ranges from July 10, when an estimated 34 percent of HY birds are thought to have fledged, to August 24, about the time when HY and AHY murrelets become indistinguishable at sea because AHY birds begin pre-basic molt (Long and others, 2001; Peery and others, 2007). Thus, we included only surveys between July 10 and August 24 to estimate annual juvenile ratios (Peery and others, 2007). Identification of HY birds followed techniques outlined by Long and others (2001) and photographs of potential HY birds taken during the survey. We included only those birds confidently identified to age class to estimate the juvenile ratio. Raw counts are used for the ratio, as opposed to estimates of density or abundance from detection function modeling, under the assumption that HY and AHY murrelets have equivalent detection functions (Peery and others, 2007).

We adjusted HY and AHY counts to account for birds expected to have been inland during the time of the survey. A certain percentage of AHY birds are still incubating young during the fledging period; therefore, are not on the water during at-sea surveys, potentially creating a positively biased juvenile ratio. The proportion, p_{A_i}, of AHY birds incubating in survey *i*, is reported to be less than 6 percent between July 10 and July 17 and less than 1 percent after July 17 (Peery and others, 2007) and estimated by linear regression model (Peery and others, 2007) as

$$p_{A_i} = 18.7145545 - 0.18445455 \times DATE_i + 0.00045455 \times DATE_i^2 \tag{1.1}$$

where

$DATE_i$ is Julian Day of survey *i*.

Therefore, to correct for the number of AHY birds counted at sea between July 10 and July 17, we calculated, as the date-corrected number of AHY individuals, A_i, as

$$A_i = \frac{A_{observed_i}}{1 - p_{A_i}} \tag{1.2}$$

where

$A_{observed_i}$ is the number of after-hatch-year (AHY) birds counted on survey *i*, and

p_{A_i} is the proportion of incubating AHY individuals during survey *i* (eq. 1.1).

For surveys after July 17, we assumed no birds were incubating, and the observed number of AHY birds was not date-corrected.

In addition to adjusting for incubating adults (to avoid positive bias in the estimated ratio), the juvenile ratio calculation can be negatively biased by not accounting for HY birds that have not yet fledged by the time of the survey. Based on 47 observed fledging events in California, Peery and others (2007) estimated the daily percentage of juveniles expected to have fledged during the study timeframe. Therefore, to adjust for the number of HY birds observed during a given at-sea survey, we calculated the proportion, p_{H_i}, of HY birds incubating in survey *i*, estimated by linear regression model (Peery and others, 2007) as,

$$p_{H_i} = -1.5433 + 0.0098 \times DATE_i \tag{1.3}$$

where

$DATE_i$ is Julian Day of survey *i*.

To correct for the number of HY birds not counted at sea because they had not yet fledged, we calculated the date-corrected number of HY individuals, H_i, as

$$H_i = \frac{H_{observed_i}}{p_{H_i}} \tag{1.4}$$

where

$H_{observed_i}$ is the number of HY individuals counted on survey *i*.

For each year, we used A_i and H_i to estimate the juvenile ratio $(\hat{R})$,

$$\hat{R} = \frac{\sum_1^n H_i}{\sum_1^n A_i} \tag{1.5}$$

where

n is the number of surveys (Levy and Lemeshow, 1991).

For each year, we estimated the variance of the date-corrected juvenile ratio, $\hat{\mathrm{var}}(\hat{R})$, following van Kempen and van Vliet [2000] and Peery and others [2007]) as

$$\hat{\mathrm{var}}(\hat{R}) = \frac{1}{n}\left(\frac{\hat{\mathrm{var}}(\hat{H})}{\hat{\bar{A}}^2} + \frac{\hat{\bar{H}}^2\,\hat{var}(\hat{A})}{\hat{\bar{A}}^4} - \frac{2\hat{\bar{H}}\,\hat{cov}(\hat{H},\hat{A})}{\hat{\bar{A}}^3}\right) \tag{1.6}$$

where

$\hat{var}(\hat{H})$ is the variance in the number of date-corrected hatch-year (HY) individuals observed,

$\hat{var}(\hat{A})$ is the variance in the number of date-corrected after-hatch-year (AHY) individuals observed,

$\hat{cov}(\hat{H},\hat{A})$ is the covariance between the numbers of date-corrected HY and AHY individuals observed,

$\hat{\bar{H}}$ and $\hat{\bar{A}}$ are the mean numbers of date-corrected HY and AHY individuals observed, respectively, and

n is the number of surveys.

We calculated date-corrected juvenile ratios and associated variance (reported as standard error and log-normal 95-percent confidence intervals) using R (R Core Team, 2016).

References Cited

Levy, P.S., and Lemeshow, S., 1991, Sampling of populations—Methods and applications (2d ed.): New York City, N.Y., Wiley, 420 p.

Long, L.L., Ralph, C.J., and Miller, S.L., 2001, A new method for ageing Marbled Murrelets and the effect on productivity estimates: Pacific Seabirds, v. 28, no. 2, p. 82–91.

Peery, M.Z., Becker, B.H., and Beissinger, S.R., 2007, Age ratios as estimators of productivity—Testing assumptions on a threatened seabird, the Marbled Murrelet (*Brachyramphus marmoratus*): The Auk, v. 124, no. 1, p. 224–240, accessed November 1, 2021, at https://doi.org/10.1093/auk/124.1.224.

R Core Team, 2016, R—A language and environment for statistical computing: Vienna, Austria, R Foundation for Statistical Computing, accessed November 1, 2021, at https://www.R-project.org/.

van Kempen, G.M.P., and van Vliet, L.J., 2000, Mean and variance of ratio estimators used in fluorescence imaging: Cytometry, v. 39, no. 4, p. 300–305, accessed January 1, 2021, at https://doi.org/10.1002/(SICI)1097-0320(20000401)39:4<300::AID-CYTO8>3.0.CO;2-O.

For more information concerning the research in this report, contact the
Director, Western Ecological Research Center
U.S. Geological Survey
3020 State University Drive East
Sacramento, California 95819
https://www.usgs.gov/centers/werc
Publishing support provided by the U.S. Geological Survey
Science Publishing Network, Sacramento Publishing Service Center

Felis and others—**Status, Trend, and Monitoring Effectiveness of Marbled Murrelet at Sea Abundance and Reproductive Output**—OFR 2023–1065

ISSN 2331-1258 (online)
https://doi.org/10.3133/ofr20231065